N71-17916
NASA CR-116422

AMERICAN SCIENCE AND ENGINEERING

11 CARLETON STREET, CAMBRIDGE,
MASSACHUSETTS 02142 (617) 868-1600

5 FEBRUARY 1971

ASE-2612

CASE FILE COPY

A PROGRAM OF X-RAY ASTRONOMY USING FOCUSING OPTICS

FINAL REPORT

REPORT PERIOD: 7 MAY 1969 TO 5 FEBRUARY 1971

CONTRACT NASW-1889

PREPARED FOR

NATIONAL AERONAUTICS
AND SPACE ADMINISTRATION
NASA HEADQUARTERS
WASHINGTON, D.C. 20546

5 February 1971 ASE-2612

FINAL REPORT

REPORT PERIOD: 7 May 1969 to 5 February 1971

A PROGRAM OF X-RAY ASTRONOMY USING FOCUSING OPTICS

CONTRACT NASW-1889

PREPARED FOR:

NATIONAL AERONAUTICS
AND SPACE ADMINISTRATION
NASA HEADQUARTERS
WASHINGTON, D.C. 20546

Approved by:

Herbert Gursky
Vice President - Research

Approved by:

Paul Gorenstein
Senior Staff Scientist

FOREWORD

The scientific objectives of this program of research and the development and performance of the instrumentation has been described in an annual report covering the period 7 May 1969 to 15 June 1970, ASE document 2474.

In the subsequent time period Rocket 13.12 CG was flown successfully. Data from that flight has been analyzed under the present contract and the results are given in this final report. Three papers have been submitted for publication and are in press. A fourth is in preparation for publication and a preliminary copy is included. This final report consists of the four preprints of those papers.

ACKNOWLEDGEMENTS

We wish to acknowledge the contribution of a few individuals in the rocket group at AS&E for the design, construction, testing and fielding of the rocket payloads. A. DeCaprio and G. Sherman were the mechanical engineers, H. Manko provided the systems engineering support, J. Ting designed a great deal of the electronics, and J. Lupone was the energetic and versatile technician who made important contributions in all phases of the effort. The rocket group was supervised by N. Guarino.

The support of the sounding rocket branch of the Goddard Space Flight Center and the U. S. Navy launch crew at the White Sands Missile Range is very much appreciated.

TABLE OF CONTENTS

Section I	"A Rocket Payload Using Focusing X-Ray Optics For The Observation of Soft Cosmic X-Rays", NUCLEAR INSTRUMENTS AND METHODS, In Press.
Section II	"Compact Source of Soft Characteristic X-Rays", REVIEW OF SCIENTIFIC INSTRUMENTS, Vol. 42, Page 166, January, 1971.
Section III	"X-Ray Structure of the Cygnus Loop", SCIENCE, In Press.
Section IV	"The Estimated Distance to Cyg X-1 Based on Its Low Energy X-Ray Spectrum", TO BE SUBMITTED TO ASTROPHYSICAL JOURNAL.

SECTION I

ASE-2489

A ROCKET PAYLOAD USING FOCUSING X-RAY OPTICS FOR THE OBSERVATION OF SOFT COSMIC X-RAYS

By:

P. Gorenstein, B. Harris, H. Gursky, and R. Giacconi

American Science and Engineering, Inc.
Cambridge, Massachusetts

Presented at:

Symposium No. 41 of I.A.U.
New Techniques in Space Astronomy
Munich (Germany) - August 10-14, 1970

TABLE OF CONTENTS

		Page
1.0	INTRODUCTION	1
1.1	General Description of the Payload	1
1.2	Sensitivity and Comparison to Non-Focusing Systems	4
2.0	DESCRIPTION OF PAYLOAD	8
2.1	Mirror Assembly	8
2.2	Detector	12
2.3	Gas Handling System	13
3.0	CALIBRATION AND OPERATION OF THE PAYLOAD	17
3.1	Radioactive Sources	17
3.2	Alignment of the Aspect Camera and Collector	17
3.3	Flight Performance	17
ACKNOWLEDGEMENTS		22
REFERENCES		23

1.0 INTRODUCTION

1.1 General Description of the Payload

Focusing x-ray optics is a powerful technique for the detection, localization, and study of the angular structure of cosmic x-ray sources. It is effective at the long wavelengths, $\lambda > 10\text{Å}$. This technique has been applied in the construction of a "focusing collector" payload, that was flown aboard an Aerobee 170 rocket on 26 June 1970. An x-ray collector that is a refinement of a design of Giacconi and Rossi, 1961, was used. A photograph of the payload and its major components is shown in Figure 1. Results from the flight indicate that the actual performance of the payload has fulfilled our expectations.

The major components of the payload are:

(1) the mirror assembly, an array of reflecting plates that focus along a line,

(2) a thin window position sensitive proportional counter in the focal plane providing eight elements of angular resolution.

In addition, there is an aspect camera that photographs the star-field through a central aperture in the mirror assembly.

The payload is primarily a survey instrument to be used in the scanning mode for the detection and localization of cosmic x-ray sources in the ultra soft region 10-80Å. The overall field of view is $2^{\circ} \times 8^{\circ}$ but the angular resolution is considerably better than this by virtue of the fact that the position sensitive counter system divides the focal plane into two groups of four elements of angular resolution, where each group of four is along the direction of focusing, and the two groups divide the other direction in half. For a strong source the location precision obtainable from a single scan is about $0.1^{\circ} \times 1^{\circ}$. As the payload is slowly rotated by the rocket

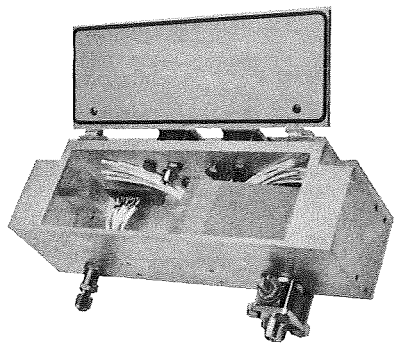

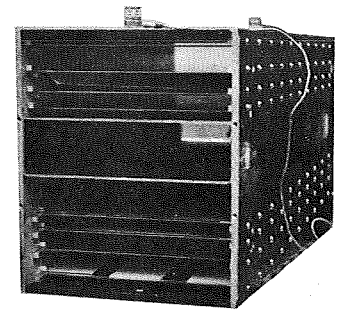

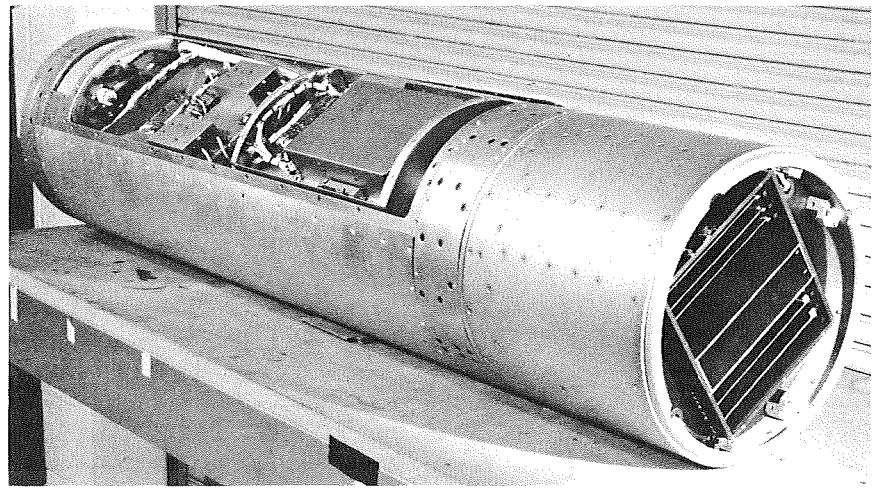

Figure 1. Photograph of rocket focusing collector payload plus view of mirror assembly and proportional counter system. Only one of the two multi-wire proportional counters is present in the vacuum box.

control system, a line image of a cosmic x-ray source moves across the detector. Events from a given celestial location can be followed from one element of angular resolution to another so that the quantity of background that accompanies a source is that amount which is detected in a single element of angular resolution in the focused dimension rather than that of the entire detector.

It is evident that focusing can result in excellent angular resolution. However, in this case, it is also true that focusing results in a very high sensitivity for detecting x-ray sources in the 10-80Å band. Focusing reduces the size of the proportional counter so that the background is low and very thin windows of high transmissibility can be used with a high degree of reliability. Low energy electrons and ions have given great difficulty to non-focusing soft x-ray detectors (Hill et al, 1970). In our configuration, they have almost no direct path to the counter so that an important source of background is essentially eliminated. Position sensitivity of the detector further reduces the residual background associated with a source by a factor that is equal to the number of elements of angular resolution. The net result is a system whose sensitivity in this wavelength band is equal to or greater than that of any other system that could be placed aboard the rocket. Fisher and Meyerott, 1966 have also constructed a somewhat similar rocket payload.

This payload differs considerably in concept from that of the very high resolution x-ray telescopes that have been used to photograph the x-ray structure of the sun (Vaiana et al, 1968). In our system the emphasis is on maximum collection efficiency rather than angular resolution. A large efficiency is attained by using

essentially flat plates as the reflecting surfaces. The virtue of flat plates is that they can be polished to a great degree of smoothness and readily can take coatings of higher Z materials. Focusing is achieved by way of a slight curvature that is introduced mechanically after the surface is polished and coated. Use of a thin window proportional counter with multi-wires as the detector assures high quantum efficiency as well as good spatial sensitivity.

Figure 2 is a schematic diagram of the collector and detector. All the x-rays from a distant source are focused onto one wire of the multi-wire counter. One or two dimensional versions of the focusing collector concept can be made. Conceptually, a two dimensional collector consists of two successive one dimensional units at 90° to each other. The one dimensional version was more appropriate for the rocket experiment because of its lighter weight and broader field of view. These features are desirable in a scanning experiment whose duration is only a few minutes.

1.2 Sensitivity and Comparison to Non-Focusing Systems

Table I summarizes the geometrical and performance characteristics of this system in comparison to those of an alternative non-focusing system for a rocket payload detecting x-ray of wavelength exceeding 44Å.

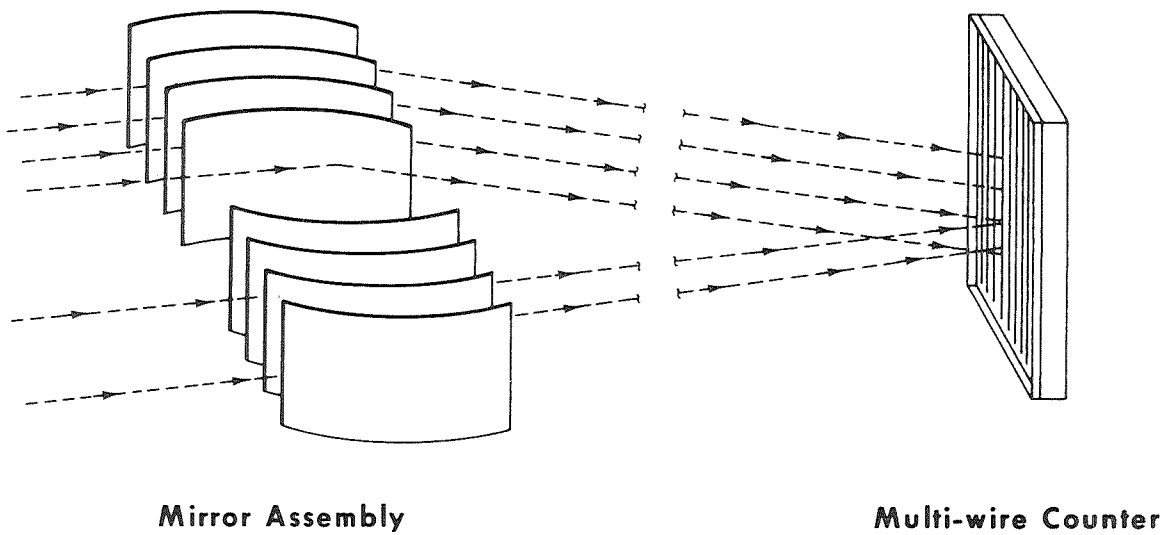

Figure 2. Schematic view of one dimensional focusing collector plus detector.

TABLE I

Comparison of Focusing and Non-Focusing Rocket Payload

Characteristic	One Dimensional, Focusing System	Typical Non-Focusing System
Field of view	$2^{\circ} \times 8^{\circ}$	$1^{\circ} \times 20^{\circ}$
Frontal area	$400 cm^2$ (nose)	$1200 cm^2$ (side)
Effective Collecting Area $\lambda > 44 Å$	$160 cm^2$	$1200 cm^2$
Total Detector Area	$100 cm^2$	$1200 cm^2$
Area Per Resolution Element	$25 cm^2$ (4 elements)	$1200 cm^2$
Relative Non-x-ray background Rate, B	1	48
Window Material	1.3μ polypropylene and support	3μ Kimfol and support
Bandwidth	44-80Å	44-64Å
Counts/sec from Crablike Source*, N (no interstellar attenuation)	1.4×10^3	3×10^3
Relative Sensitivity, $N/\sqrt{B}$, $\lambda > 44 Å$	3	1

*$dN/dE = 9 E^{-2}$ photons/cm^2-sec-Kev

In a background limited situation the focusing system will have superior sensitivity for detecting sources. The superiority is based on two factors: (1) reduced background in a smaller detector, and (2) use of a thinner entrance window on the proportional counter. For a fixed experiment size the addition of more elements of angular resolution will further enhance the sensitivity of the focusing system while there are no simple changes that will add to the sensitivity of the non-focusing system.

The optical design of the collector involves certain trade-offs between effective area, bandwidth, and field of view. If the focal length is shortened, x-rays will be reflected through large angles. As a result the collector is effective only at the longer wavelengths, say $\lambda > 44$Å. On the hand, the total field of view of the collector is larger and fewer plates (less support structure) are needed to fill the aperture. As a result the area time factor of a single scan is larger at the longer wavelengths, at the expense of the shorter wavelengths. The collector used in this payload was designed to be sensitive down to wavelengths of about 10Å. This would enable us to compare our results with previous observations in the 1-10Å range.

A computer code has been written to facilitate the design of one and two dimensional focusing collectors. For a given focal length and plate thickness the program will determine the geometrical properties of all the parabolic plates needed to fill a given aperture and on the basis of ray tracing calculate the effective collection area as a function of wavelength at each angle of incidence (VanSpeybroeck and Chase, 1970). In the absence of detailed measurements of the spectral reflection efficiency the results of the program are needed for interpreting spectral data from cosmic x-ray sources.

2.0 DESCRIPTION OF PAYLOAD

2.1 Mirror Assembly

Figure 3 is a schematic view of the rocket payload.

This payload's collector consists of eight parabolic plates having a common focus and allowing no direct path of on-axis radiation to the detector. The plates are fabricated from .040" sheets of commercial float glass measuring 8" x 16". A .020" steel backing is bonded to the glass with RTV adhesive for mechanical strength. Following a procedure used by the Columbia University group in a different type of collector a 1500Å layer of chromium was evaporated onto the glass surface by a commercial manufacturer. The resulting surface retains the original smoothness of the glass and has improved reflection properties at the shorter wavelengths. The reflecting plates were mounted inside of an aluminum box and constrained to follow the correct parabolic curves by a set of accurately placed contact pins at the top and bottom. A serious limitation to most commercial varieties of float glass is that although the surfaces are smooth, they are not free of ripples. Figure 4 illustrates the imaging properties of the collector to a collimated beam of light. It is seen that the image has a considerable width, approximately 0.3". Part of this spread can be attributed to the ripples on the glass surface and the rest to imperfect registration and alignment of the plates. Although the angular resolution of the collector is far below what can be achieved in principle, it was adequate for the rocket experiment.

The theoretical effective area of the rocket collector as a function of wavelength and angle is shown in Figure 5. The calculation

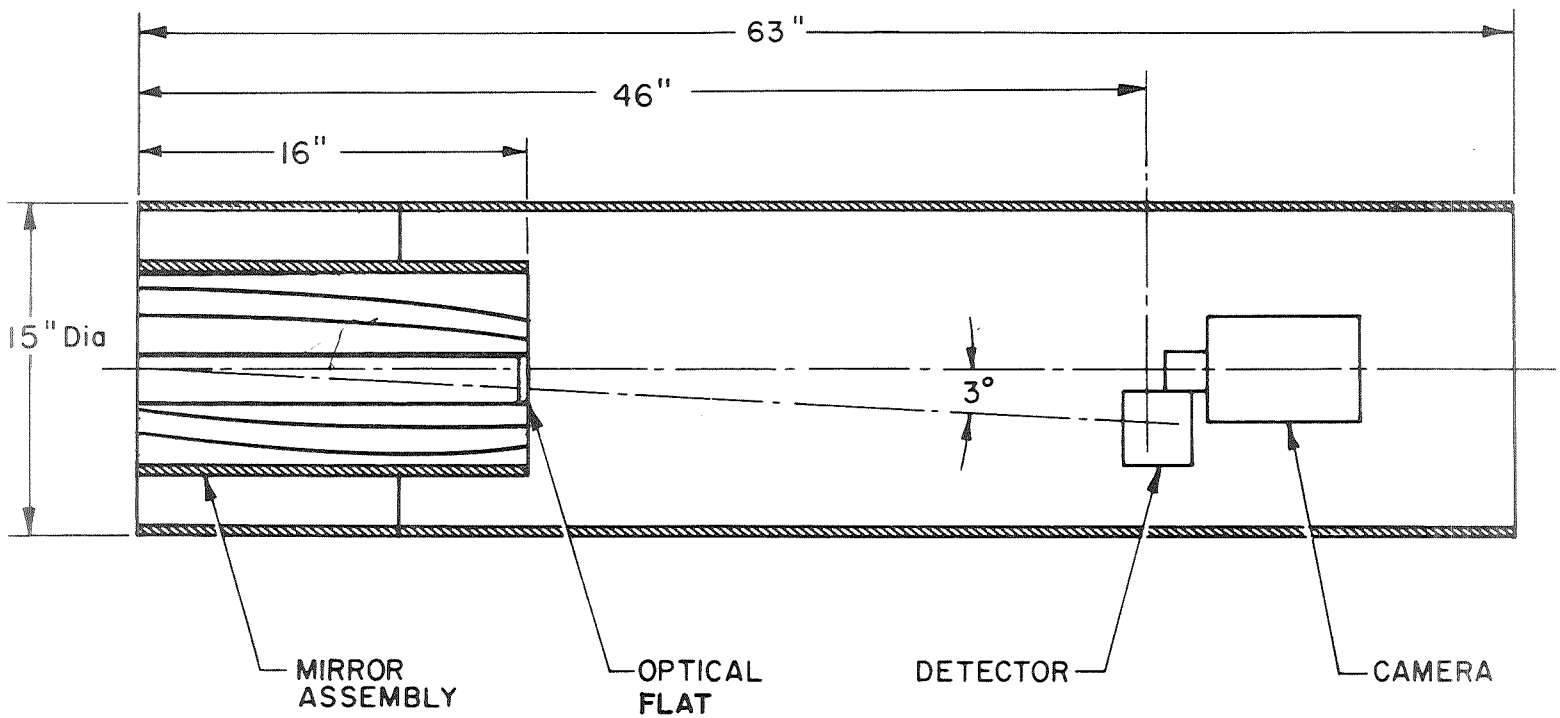

Figure 3. Schematic view of rocket payload.

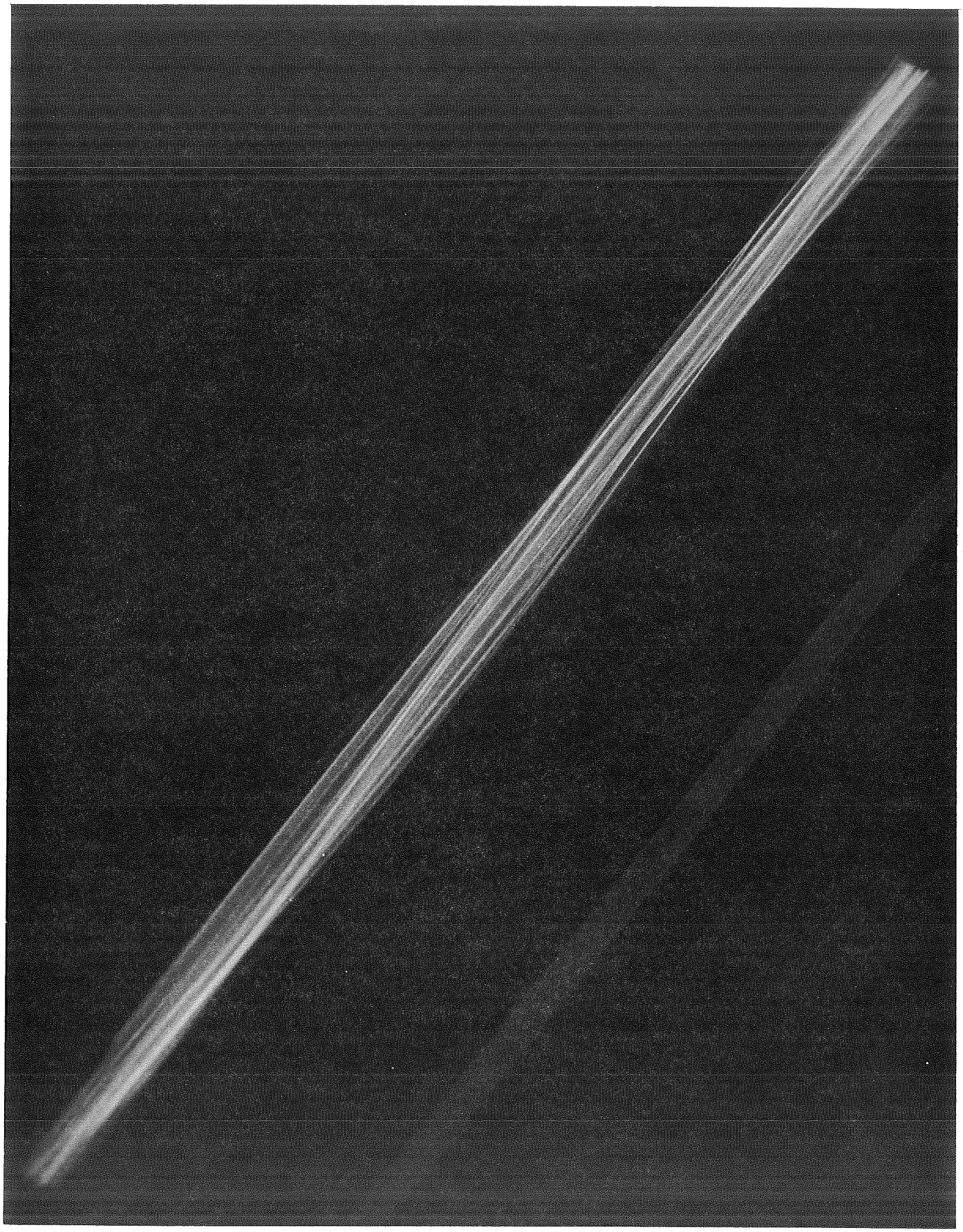

EK-013

Figure 4. Visible light image cast by focusing collector. Rather large width is a result of ripples on reflecting surfaces and imperfect plate alignment.

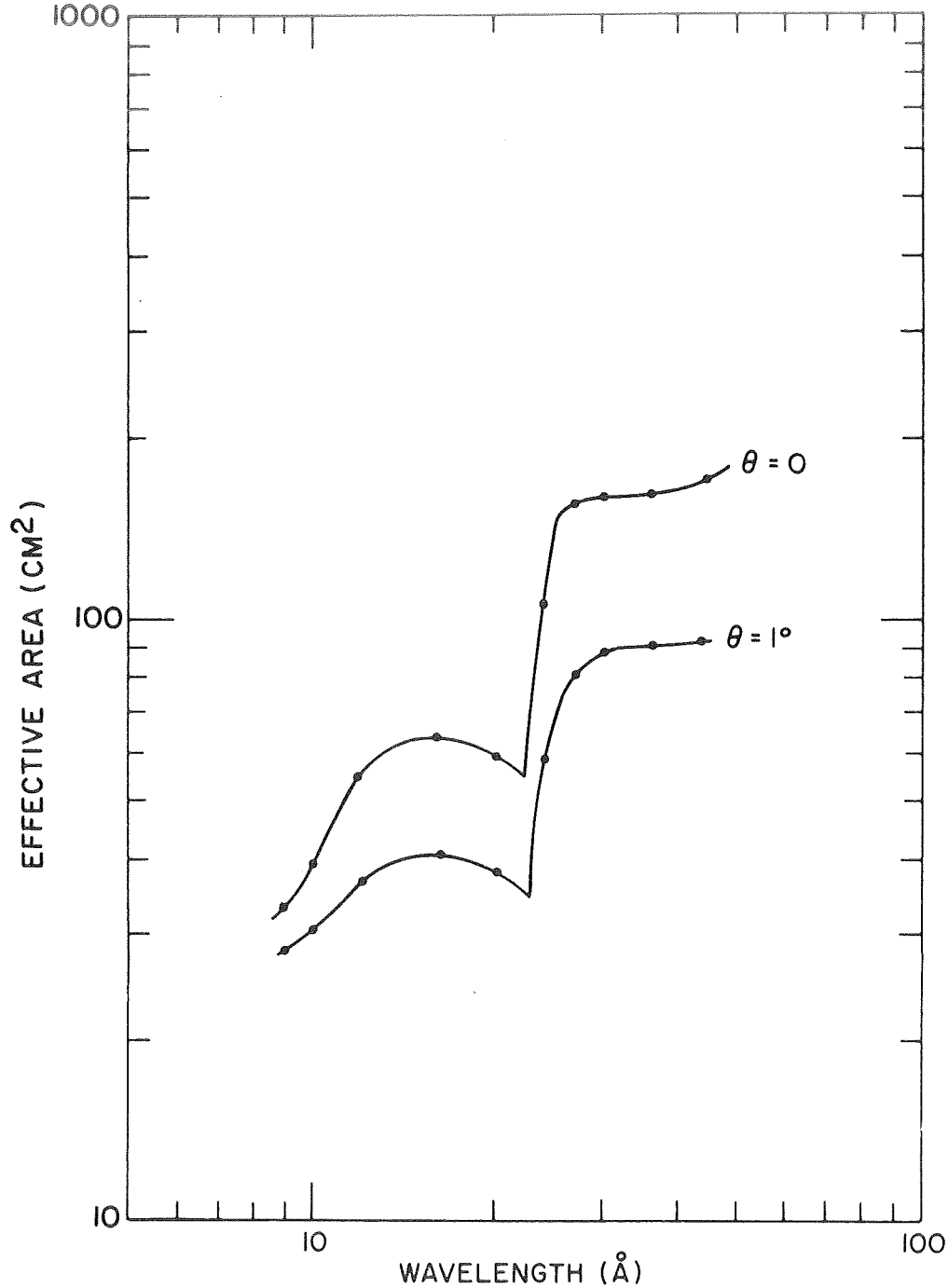

Figure 5. Effective area of focusing collector as calculated by ray tracing program. Grazing incidence reflection probabilities, vignetting, and loss at non-reflecting structures are included.

predicts a large dip in effective area at the L edge of chromium. The calculation was done by the ray tracing program and includes the angular dependent reflection probability, vignetting, and the loss of x-rays at non-reflecting structures. Laboratory measurements of the effective area at 10Å was in reasonable agreement with the theoretical values.

2.2 Detector

For reasons of redundancy and improved angular resolution two multi-wire proportional counters served as the detectors. Each unit contained four active wires separated from each other by wires at ground potential. The four active wires divided the 2° field of view in four equal parts. Counts originating from a cosmic x-ray source of small angular size will be collected instantaneously onto only one of the wires while the other wires can observe other sources or measure background. The use of two identical units provided angular resolution along the non-focusing 8° direction by virtue of the fact that the collector acts as a conventional collimator. Effectively, their field of views in the 8° direction are offset so that on source the ratio of their counting rate is a function of angle.

The entrance window of the detector was polypropylene with a carbon coating to reduce ultra-violet transparency and provide a conductive inner surface. The polypropylene had been stretched down to a thickness of about 1.3 microns from a commercial thickness of .001" using a technique of the Columbia University group. Measured x-ray transmission of the material after stretching and coating was 72% at 44Å. A 64% transparent coarse-fine strong mesh supports the window against an outward pressure differential when the counter is operated in vacuum. Propane at a pressure of 50cm of Hg was the proportional counter gas. A 0.5" depth results

in good x-ray efficiency over the entire wavelength range. Propane has a fairly good resolution response to x-ray sources of various wavelengths as is shown in Figure 6. Figure 7 shows the net effective area of the entire system as a function of wavelength for x-rays that are normally incident to the collector.

2.3 Gas Handling System

Figure 8 shows the gas handling system for the proportional counters. The major items were a trap to prevent liquid propane from entering the counters, a two stage gas pressure regulator, a controlled leak in each counter that was large compared to the natural window leaks. The function of the leaks was to bias the flow system at a stable operating point. The propane supply of the payload was sufficient for 45 minutes of normal operation. Both detector units were seated inside a protective vacuum tight box which was opened in flight by a timing signal. For testing and calibration purposes the box could be conveniently evacuated by a small fore pump. This feature enabled us to test and calibrate the counters at its normal operating pressure with radioactive sources directly in the payload at any time.

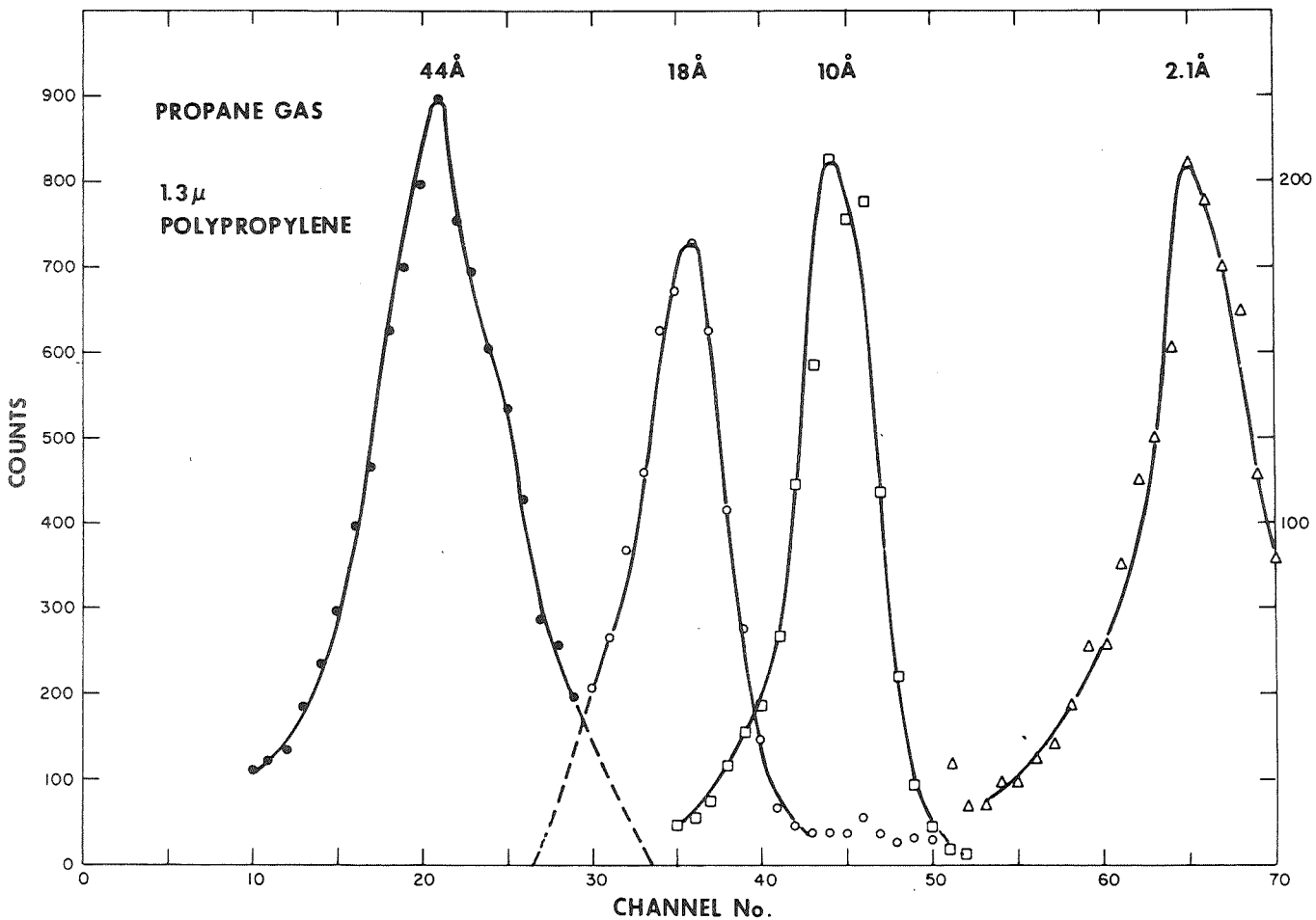

Figure 6. Pulse height analyzer spectra of multi-wire counter when irradiated with various characteristic x-ray lines. Horizontal scale is made intentionally non-linear to accommodate a large dynamic range.

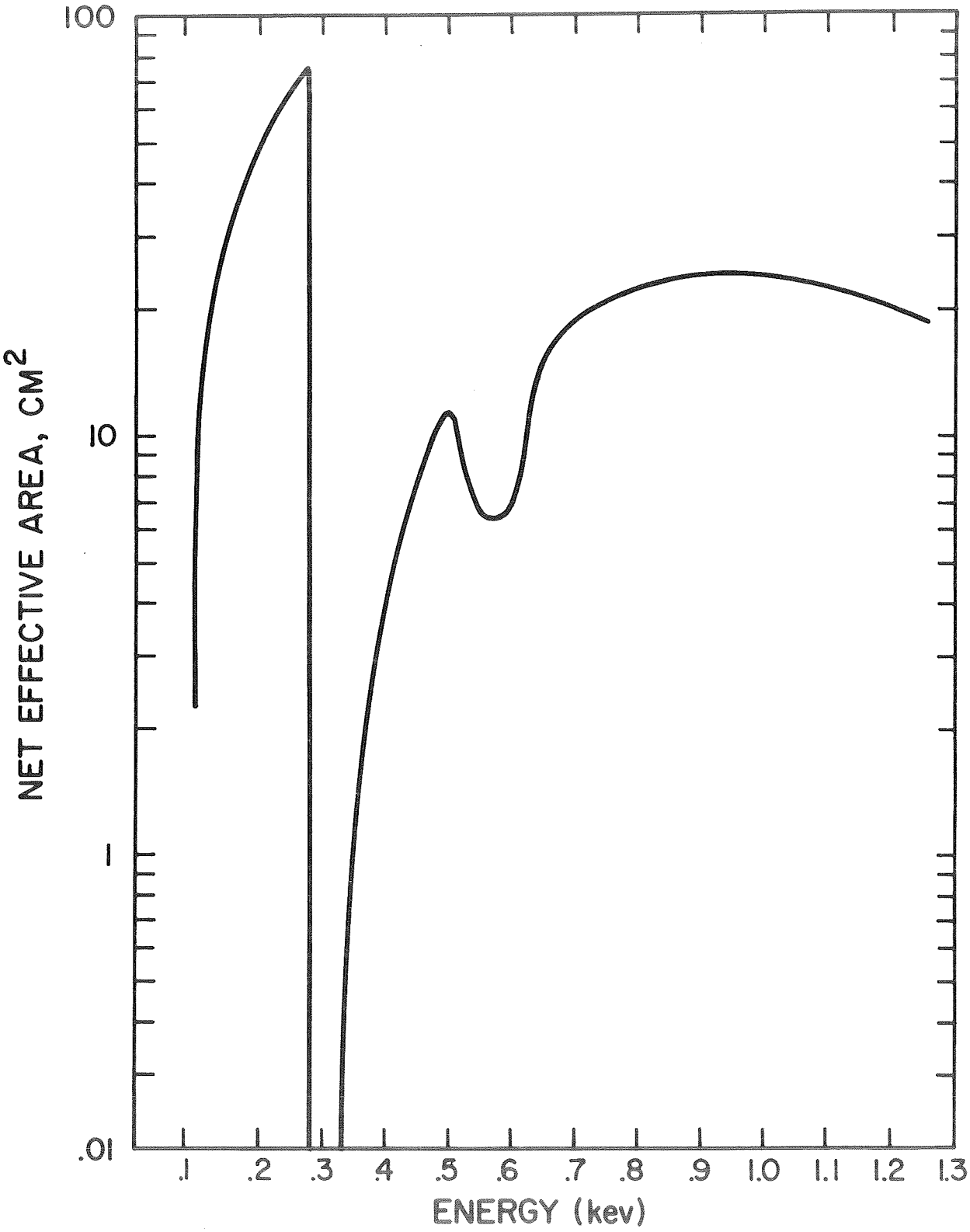

Figure 7. Net effective area of focusing collector payload for on-axis x-rays. All known efficiencies are included.

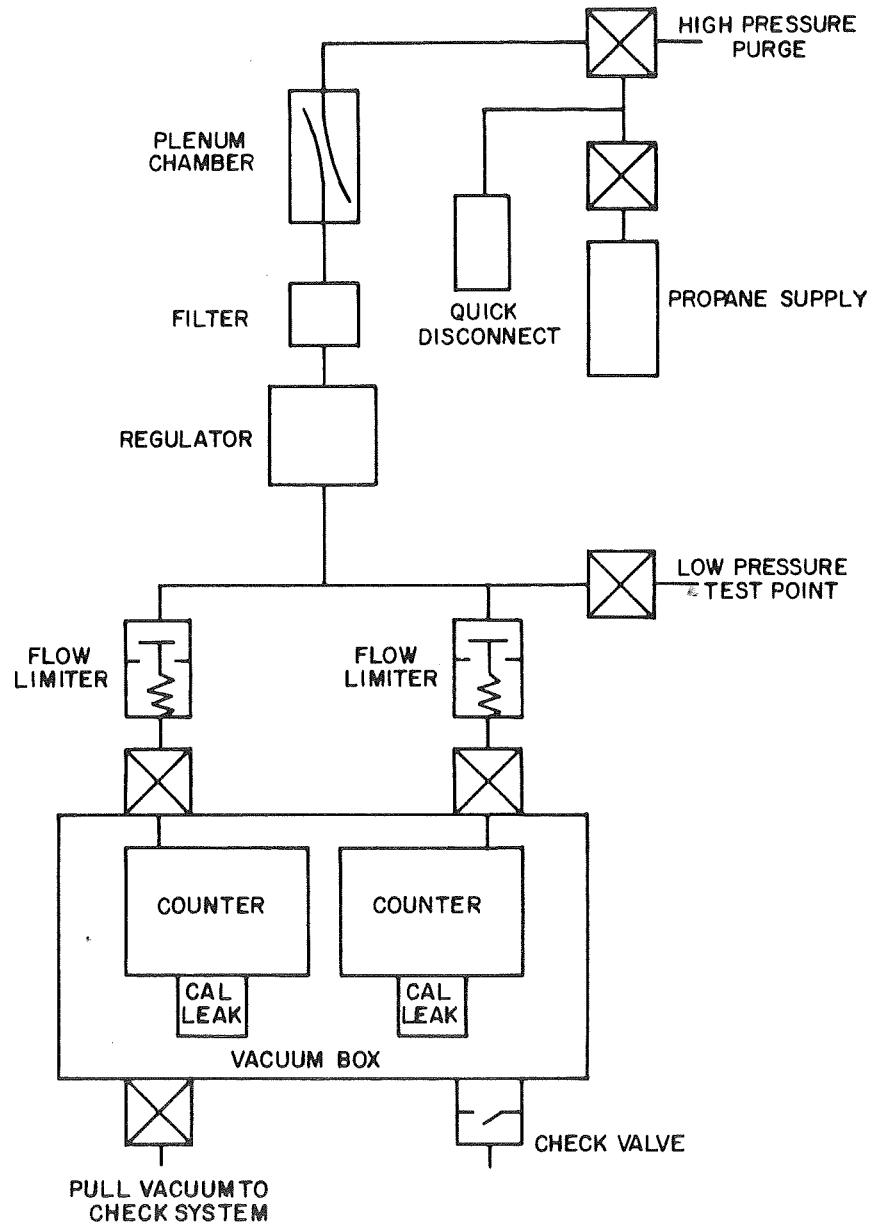

Figure 8. Block diagram of system used to supply propane gas to the two detector units.

3.0 CALIBRATION AND OPERATION OF THE PAYLOAD

3.1 Radioactive Sources

Radioactive sources proved to be a very convenient method of calibrating the proportional counters. Characteristic x-ray lines of light elements such as B, O, F and Mg were produced by α particle excitation. The source geometry is shown in Figure 9. When a 300μc Po^{210} source is used in this configuration the yield of photons is in the range 10^2 - 10^3 per second.

3.2 Alignment of the Aspect Camera and Collector

A 250-foot vacuum facility was used to test the total performance of the payload. A small visible x-ray source placed at that distance was the test object. The payload was placed on a rotary table whose angular rotation could be controlled and read out remotely to a precision of about an arc-minute. As the angular position of the table was incremented the payload operated normally. In this manner the relative alignment of the aspect camera and the collector-counter system was measured to a precision of a few arc-minutes.

3.3 Flight Performance

On June 26 the payload was flown at the White Sands Missile Range aboard an Aerobee 170 rocket. The payload scanned a portion of the constellation of Virgo plus a region in Cygnus. Preliminary analysis of the data indicates a soft x-ray source in Cygnus of finite angular extent. This is undoubtedly the same source observed by Henry et al, 1968 and Grader et al, 1970. Its finite angular extent as seen by us and Grader et al, plus the preliminary aspect data suggest that the object is a supernova remnant known variously as the Cygnus Loop and the Veil Nebula. Figure 10 shows the data from the source in comparison to

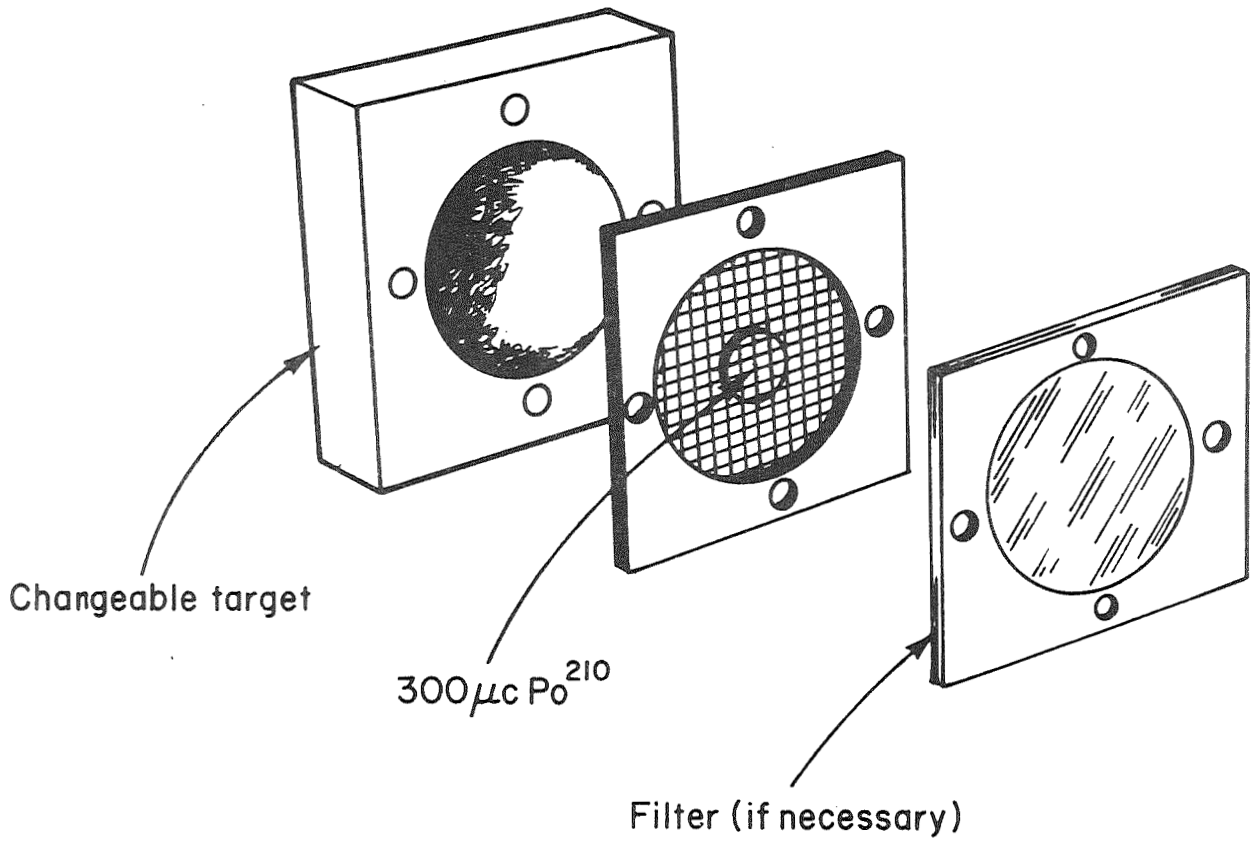

Figure 9. Alpha fluorescence source with changeable targets used to produce characteristic lines of light elements.

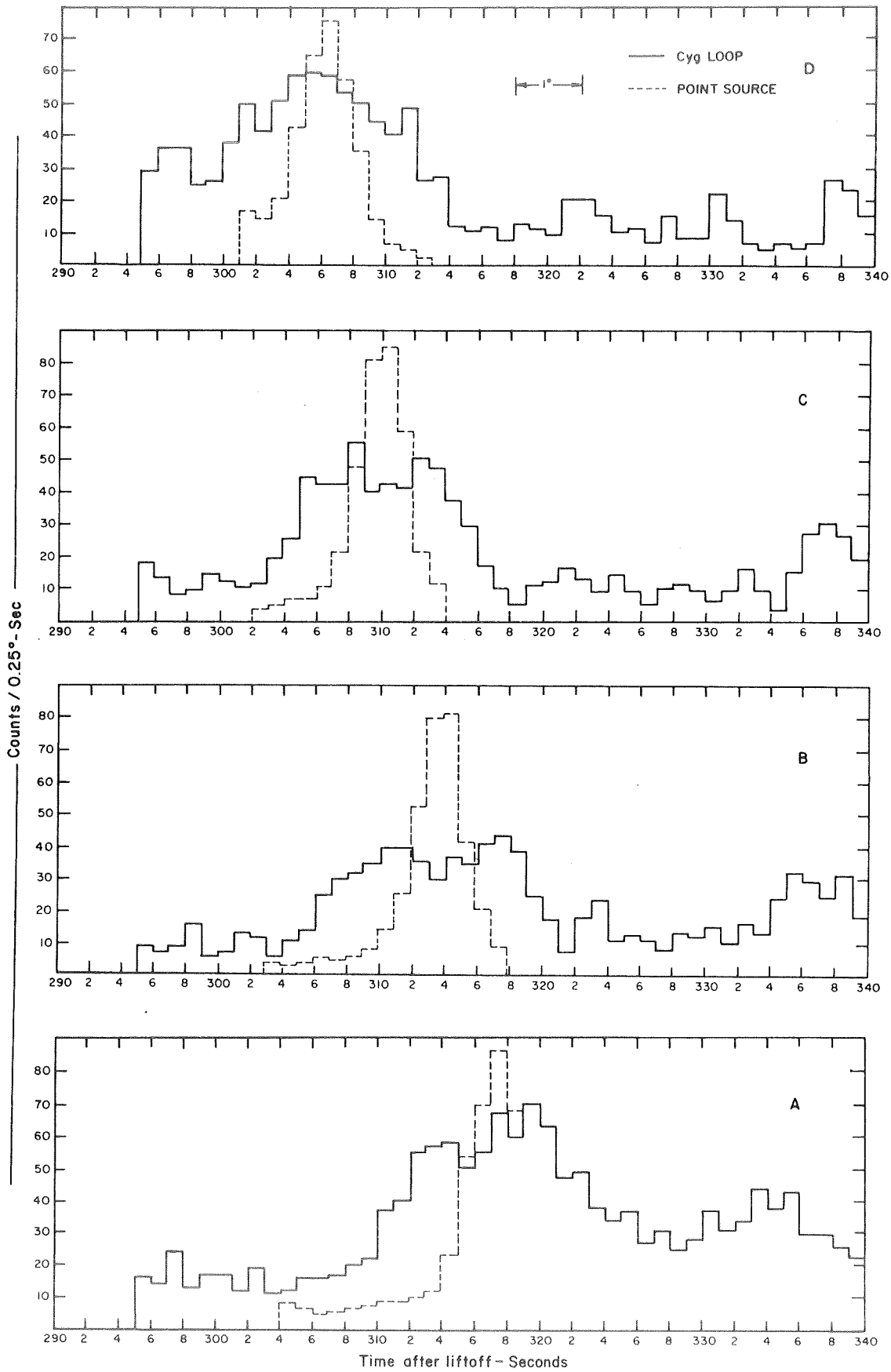

Figure 10. Observation of the Cygnus Loop. Dotted lines are the response of the system to a point source of soft x-rays at a distance of about 250'.

measurements obtained with a point source at the long vacuum facility. Events from the two counters that are offset in the 8° direction are summed as one detector. These data have been refined by the inclusion of several background reduction techniques in the data analysis, and are reported in some detail elsewhere (Gorenstein et al, 1970). However, on the basis of the previously reported strength for the Cygnus Loop these results do imply that the net efficiency of the system is comparable the expected value.

The relative insensitivity of this instrument to soft particles as compared to a conventional payload is illustrated in Figure 11. Data from only one of the detector elements representing one - eight of the total number of events from the Cygnus Loop are shown. It is evident that this signal-to-noise ratio is very much improved in the focusing case.

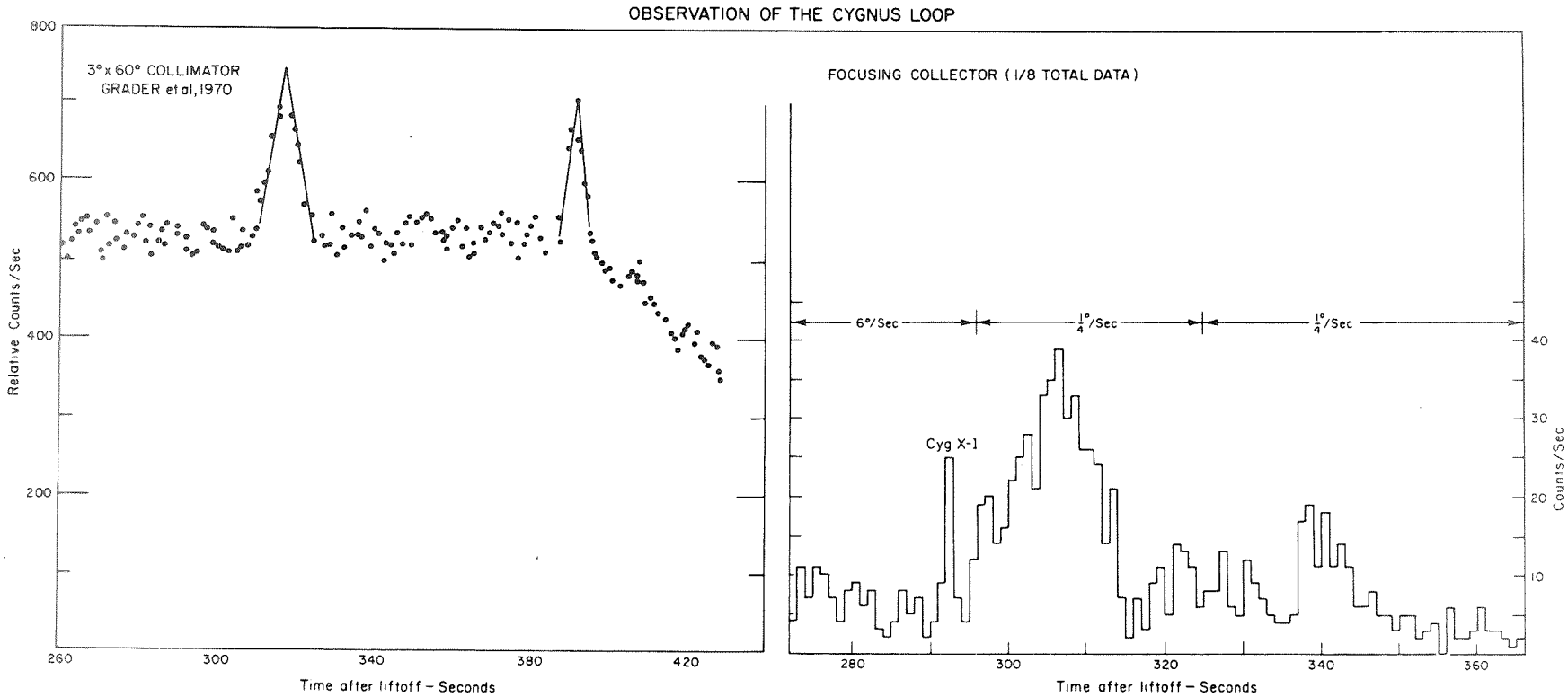

Figure 11. Observation of x-rays from Cygnus Loop by a conventional collimator payload and by the focusing collector described in this report. Data from only one of the eight focal plane counters of the collector are shown. The signal-to-noise ratio is very much greater in the case of the focusing collector due to its relative insensitivity to the soft particles which account for most of the background in the collimator observation. (The second Cygnus Loop peak is suffering air attenuation as the rocket falls.)

ACKNOWLEDGEMENTS

We would like to acknowledge the aid we received from Professor R. Novick and Professor P. Vandenbout of Columbia University concerning techniques for preparing chromium coated surfaces and polypropylene windows for the counters. We would like to thank Professor G. Garmire of Cal Tech for some informative discussions concerning the gas handling system. Dr. P. Bjorkholm of ASE contributed to the development of this payload.

A. DeCaprio, G. Sherman and H. Manko of ASE provided the engineering support needed for the design and construction of this payload. This work was supported by the National Aeronautics and Space Administration under contract NASW-1889.

REFERENCES

Fisher, P.C., and Meyerott, A.J., (1966), I.E.E.E. Trans. Nuc. Sci. NS-13 580.

Giacconi, R., and Rossi, B., (1961). Application filed with U.S. Patent Office, February 23, 1961. Patent No. 3, 143, 651 awarded August 4, 1964.

Gorenstein et al, 1970, "Soft X-rays from the Cygnus Loop", to be published.

Grader, R.J., Hill, R.W., and Stoering, J.P., (1970), Ap.J. (Letters) 161, L45.

Henry, R.C., Fritz, G., Meekins, J.F., Friedman, H., and Byram, E.T., (1968), Ap.J. (Letters) 153, L11.

Hill, R.W., Grader, R.J., Seward, F.D., and Stoering, J.R., (1970), UCRL-72011 (submitted to JGR).

Vaiana, G.S., Reidy, W.P., Zehnpfennig, T., VanSpeybroeck, L., and Giacconi, R., (1968), Science 161, 564.

VanSpeybroeck, L., and Chase, R., 1970, "Orthogonal Mirror Telescopes for X-ray Astronomy", to be published.

SECTION II

ASE-2493

COMPACT SOURCE OF SOFT CHARACTERISTIC X-RAYS

P. Gorenstein and B. Harris

American Science and Engineering, Inc.
Cambridge, Massachusetts

ABSTRACT

A compact source of characteristic soft x-rays has been made by using alpha particles to fluoresce light elements such as boron, carbon, and magnesium. The x-ray wavelengths are varied by changing targets. Output intensities are in the range 10^2 - 10^3 photons/sec when 300μc of Po^{210} are used.

COMPACT SOURCE OF SOFT CHARACTERISTIC X-RAYS

Alpha particle induced fluorescence has been applied to the design of a versatile source of soft x-rays that can be used very conveniently to test quantum detectors. The source has proved to be very useful in the calibration of x-ray proportional counters at very long wavelengths. Characteristic x-rays of the light elements such as 67Å(B), 44Å(C), 18Å(F), and 10Å(Mg) radiation plus shorter wavelengths may be produced by selecting the appropriate target material.

Figure 1 illustrates the source geometry. The changeable targets are made by milling a spherical cap upon one surface of a rectangular block that measures 2" x 2" x 0.5". A small alpha particle source is placed at the center of the milled surface upon a transmissive supporting frame with its active side facing the target. Alpha particles impinge upon the spherical surface and induce emission of characteristic x-rays over a broad angular range. It is desirable to have the alpha source as small as possible to minimize its shadowing of the fluorescence radiation. In our case it was 1/4" diameter. There is provision for an absorbing filter on the outside of the alpha source that acts upon the outgoing x-rays. This feature is useful when complex targets containing several elements are used. In those cases the filter material can be selected on the basis of its K absorbing edge to suppress lines that predominate too strongly.

We have used targets of boron nitride, carbon, teflon, and magnesium. A filter consisting of a thin layer of amorphous boron applied to a one micron substrate of polypropylene has been used to attenuate the strength of the carbon line from

teflon so that it would appear about as strong as the fluorine line in our detectors.

With a source strength of 300μc Po^{210} the yield of characteristic x-rays is in the range 10^2 - 10^3 per second depending on the target material. We do not detect any x-ray continuum and the number of backscattered alpha particles is negligibly small. If Am^{241} is substituted for Po^{210} there appears an appreciable component of backscattered gamma rays which was very undesirable in our case. It is possible that the output of fluorescence x-rays can be increased significantly by lowering the energy of the alpha particles. In all of the above cases the range of the alpha particles in the target material is much larger than the mean free path for the absorption of outgoing fluorescence radiation. Inherent to the ionization process is the property that more energy is lost by a charged particle as it slows down. Hence with the emission of alpha particles at nearly the full energy, a large part is dissipated at too great a depth into the target. If a thin absorber is placed over the alpha source it should result in more efficient utilization of the energy and larger x-ray yields.

Thinly coated alpha sources of high specific activity such as the one described here have a tendency to suffer mechanical deterioration with time. This is especially true when they are subjected to many vacuum cyclings. We have observed an alpha source covered with 1/4 mil mylar to eventually leak activity. Another source covered with about 1/2 mil beryllium is still intact after about 10^2 vacuum cyclings. Inasmuch as degradation of the alpha energy can increase the x-ray output up to a point it is advantageous to place relatively thick beryllium coverings over the source.

The characteristic x-ray source has been used to calibrate the proportional counters of an x-ray astronomy rocket payload. The compactness and portability of the source made it especially useful for calibrating the counters in the field prior to launch. Figure 2 shows the response of one counter to a teflon target and a magnesium target as seen in a pulse height analyzer. Lines at 44Å, 18Å, and 10Å are evident. The widths of the analyzer peaks are consistent with pure lines and the expected resolution of the proportional counters.

This work was supported by the National Aeronautics and Space Administration under contract NASW-1889.

Figure Captions

Figure 1. Arrangement of characteristic x-ray source. The alpha source is attached to a high transmission screen.

Figure 2. Emission of characteristic x-ray source as observed in thin window proportional counter and pulse height analyzer. Lines of 44Å and 18Å are from a teflon target (CF_2). The 10Å line is from a magnesium target. The horizontal scale is non-linear intentionally for reasons relating to the operation of the proportional counters in a rocket payload.

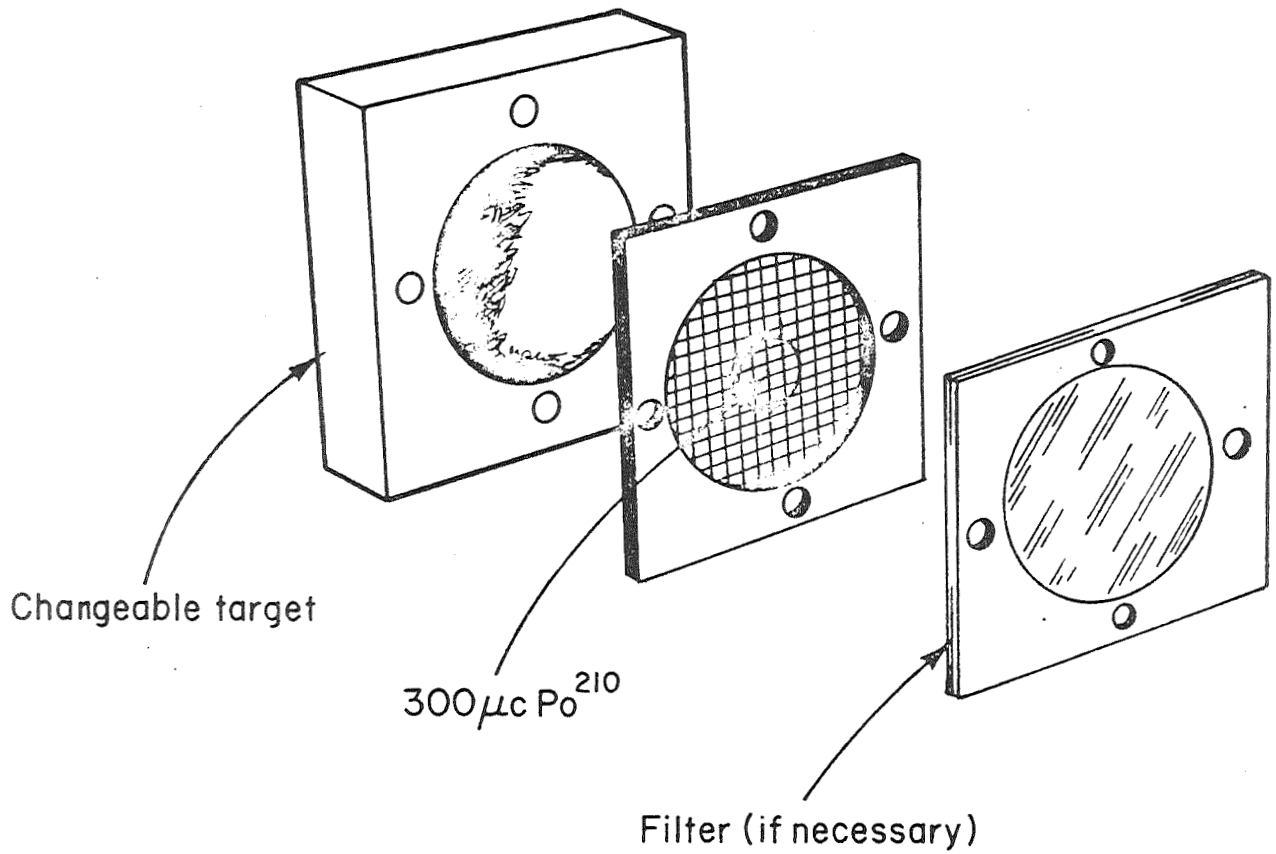
Changeable target
300 μc Po210
Filter (if necessary)

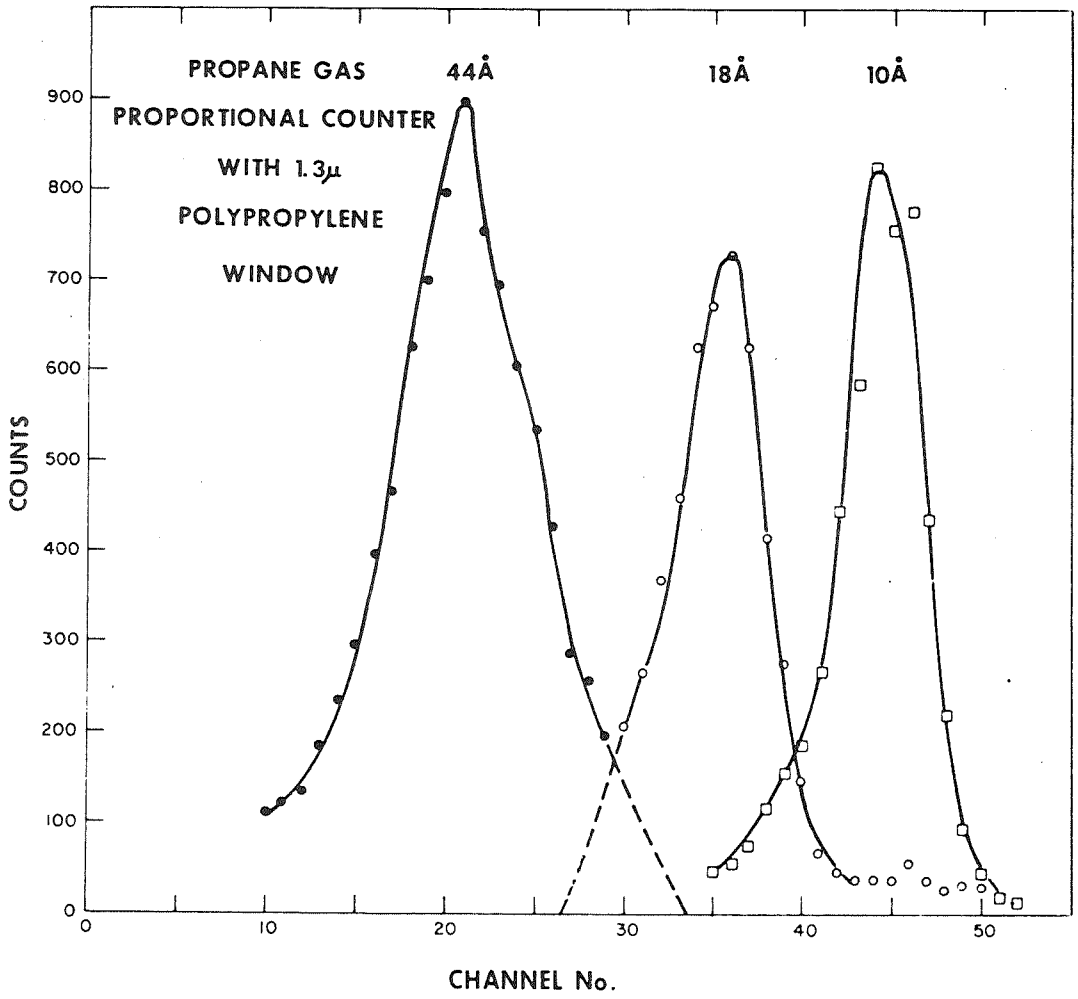
PROPANE GAS
PROPORTIONAL COUNTER
WITH 1.3μ
POLYPROPYLENE
WINDOW
44Å
18Å
10Å
COUNTS
900
800
700
600
500
400
300
200
100
0
0
10
20
30
40
50
CHANNEL No.

SECTION III

ASE-2539

X-RAY STRUCTURE OF THE CYGNUS LOOP

P. Gorenstein, B. Harris, H. Gursky, R. Giacconi
American Science and Engineering, Inc.
Cambridge, Massachusetts 02142

and

R. Novick and P. Vanden Bout
Columbia Astrophysics Laboratory
Columbia University, New York, New York 10027

ABSTRACT

X-ray emission from the Cygnus Loop was observed in the energy region .2 - 1keV with a collector that focused x-rays along one dimension while scanning across the nebula. The total integrated intensity is 1.3×10^{-8} ergs/cm^2-sec. The one dimensional x-ray structure has the same angular size $\sim 3^{\circ}$ as the outermost boundaries of the optical filaments. There is no increase in x-ray emission at the center of the nebula nor at the strong feature that is seen in certain radio maps. The x-ray spectrum is consistent with thermal radiation from a hot plasma at a temperature of about 4×10^{6} $^{\circ}$K with evidence for a line at 19Å corresponding to the 2P→1S transition of OVIII.

X-ray emission from the supernova remnant known as the Cygnus Loop or Veil Nebula was observed in the energy range .2 - 1keV from an attitude controlled Aerobee 170 sounding rocket that was launched 4:55UT on 26 June 1970 from the White Sands Missile Range. A recent article by Grader, Hill and Stoering(1) has reported intense x-ray emission in this range from an extended object which they identified with the Cygnus Loop. Also this object is very likely coincident with the x-ray source Vul XR-1 which had been reported previously with an imprecise location(2).

The purposes of this observation were to: 1. obtain a precise location that would confirm the identification by Grader et al of the extended x-ray source with the Cygnus Loop; 2. obtain a high resolution mapping of the x-ray emission that could be correlated with the optical and radio pictures of the Cygnus Loop; 3. distinguish between a thermal and non-thermal mechanism on the basis of a spectral analysis of the x-ray data.

A rather unique instrumentation system based on focusing x-ray optics by means of grazing incidence reflection was used in this observation. For x-ray wavelengths exceeding 10Å, the potential advantages of focusing compared to conventional systems are better angular resolution and an improved ratio of signal-to-noise by virtue of the fact that the focused image is considerably smaller than the collecting area. Hence, the detector can be small and less influenced by cosmic ray effects. Also the reflecting surfaces effectively block the direct path of soft charged particles that are sporadically present in the space environment. These particles would otherwise penetrate the thin entrance window of the detector and add to the background level. This particular instrument consists of a collector that focuses radiation in one dimension upon a multi-element x-ray detector in the focal plane. The collector consists of eight nested reflecting plates whose dimensions are 20cm x 40cm and is symmetric about the central plane. Each plate is curved slightly to approximate a parabola in one dimension and focuses to a common line. The overall field of view of the instrument is

2° along the direction of focusing and 9° along the perpendicular direction.

The eight reflecting surfaces are commercial 1mm thick float glass overcoated with an evaporated layer of 1500Å of chromium for improved x-ray reflectivity at short wavelengths and are reenforced by a steel backing. The focal plane detector is two - four wire proportional counters with an entrance window of 1.3 microns of polypropylene. The wires were spaced at a distance equivalent to an angular separation of 0.5° which determines the angular resolution of the system. A regulated supply system of pure propane gas compensated for losses through the thin polypropylene windows by maintaining the pressure at a constant level of 50cm. of Hg. The energy resolution of the detectors gave a full width at half maximum in the pulse amplitude distribution of 100% for photon energies (wavelengths) of .28keV (44Å) and about 40% at 1.25keV (10Å). The entire system is sensitive in the wavelength bands 80 - 44Å (.16 - .28keV) and 20 - 10Å (.6 - 1.2keV). Photography of the star field at intervals of one second provided the aspect data. More instrumentation details are described elsewhere(3).

This observation took place during the later phases of the rocket flight prior to reentering the earth's atmosphere. X-ray data from other regions of the sky will be reported separately. Approximately 1500 net counts were obtained during a single scan across the Cygnus Loop that took place at a rate of $1/4^{\circ}$/second. Figure 1 shows the angular response of four independent detectors to the Cygnus Loop plus, for purposes of comparison, the response to well collimated radiation in the laboratory. With the aspect information count data from the four detectors can be properly combined and represented in celestial coordinates. The result is a one dimensional x-ray map of the Cygnus Loop that is shown superimposed upon a photograph of the optical filaments in Figure 2.

Several conclusions follow from a comparison of these maps. One, the size and structure of the x-ray emission is consistent with that of the shell-like region bounding the optical filaments. The diameter of the x-ray region is about 2.8°, like that of the outermost boundaries of the filaments. There is no increase in x-ray emission at the center of the nebula. Two, to within the resolution of the instrument, $1/2^{\circ}$, the level of x-ray emission declines rather sharply at the outer boundaries of the optical filaments. Three, the strong central feature that appears in a radio contour map(4) does not coincide with a strong maximum in the x-ray emission.

A spectral analysis was made of the pulse amplitude distribution of the counts from the Cygnus Loop. The usual procedure was followed; an assumed function of energy containing undetermined parameters is multiplied by all the known efficiencies and is convolved with a resolution function that simulates the pulse amplitude distribution response of the proportional counter to mono-energetic photons at any energy(5). For each set of parameter values the degree of agreement between the computed and observed pulse amplitude spectra is decided quantitatively on the basis of a minimum chi-square test. Grazing incidence telescopes require a correction for an energy dependent x-ray reflection efficiency. A theoretical efficiency function was computed for this particular instrument from the reflection properties of chromium as measured by Ershov, Brytov, and Lukirskii(6). The theoretical telescope efficiency was confirmed at 1.25keV by laboratory measurements.

At the estimated distance to the Cygnus Loop, 770pc(7), the opacity of the galaxy becomes significant for x-ray energies, E, less than 0.3keV. In the analysis a set of x-ray attenuation coefficients for the interstellar medium as recently computed by Brown and Gould(8) for revised helium and neon abundances were used to calculate $Tr(E, N_H)$, the interstellar transmission. The value of N_H, the number of hydrogen atoms along the line of

sight was left as an undetermined parameter. The large volume of the Cygnus Loop precludes any internal absorption.

Two classes of spectral functions multiplied by interstellar transmission were considered:

(a) $$dN/dE = A\,Tr(E,\ N_H)\,E^{-\alpha}$$

(b) $$dN/dE = A\,Tr(E,\ N_H)\ \left\{Exp\ (-E/kT)/E + B\ \ \delta\,(E - .65keV)\right\}$$

The quantities α, T, N_H, B, and A are the undetermined parameters. The two expressions represent alternative physical processes resulting in x-ray emission.

Expression (a) represents the type of spectrum that could be produced by synchrotron radiation, for example, the Crab Nebula. Expression (b) is an approximation to the thermal emission spectrum that one expects from a hot plasma that contains a cosmic elemental abundance. The actual spectrum would consist of a continuum plus a number of lines and recombination edges. It has been suggested that a line at 0.65keV corresponding to the 2P→1S transition of OVIII would be a prominent feature of the thermal x-ray emission from the boundaries of a shock wave that has been produced as a result of a supernova explosion expanding into the interstellar medium(9). We represent this feature by a delta function in expression (b).

The results of the analysis show that expression (a) is inconsistent with our data for all possible values of the spectral index, α. However, one can probably not exclude more complex expressions that might arise from synchrotron radiation, for example, a power law spectrum that is characterized by a large change in the spectral index between 20 and 15Å.

Expression (b) did fit the data with an acceptable value of the chi-square with a finite value for the strength of the line at 0.65keV (the quantity "B"). Since (b) is only an approximation to the actual spectrum of radiation from a hot plasma the temperature found as a result of fitting this expression is not necessarily the same as the true temperature of the plasma. The observed and computed pulse height distributions are shown in Figure 3. The parameters associated with the best (minimum chi-square) fit are:

$T = 4.3 \times 10^6 K$

$N_H = 2.6 \times 10^{20}$ H atoms/cm^2

Total Integrated Intensity = 1.5×10^{-8} ergs/cm^2-sec $E > .2$keV.

The most outstanding result of the analysis is that about one-third of the energy flux from the Cygnus Loop for $E > .2$keV is contained in a line at 0.65keV. If true, it is rather firm evidence that the source of the x-ray emission is a hot plasma and for the existence of high temperatures in old supernova remnants. Hence, it is important to examine this result rather carefully. Inspection of the raw pulse height data from the Cygnus Loop shows that there are a large number of counts between .55 and .75keV. This results in the line at .65keV in the analysis. This feature is not questionable on the basis of its statistical significance. If spurious it originates in systematic errors. The most important possible systematic errors are: incorrect reflection efficiency of the collector, and an incorrect energy calibration of the proportional counters. Both these effects would be confined to the region around .65keV as the other parameters we determine for the Cygnus Loop spectrum are in agreement with reference (1). As for the first effect it is true that the x-ray reflection efficiency of the

chromium collector is undergoing large changes in the vicinity of the chromium L -edges. However, actual experimental values of reflectivity including edge effects as measured by Ershov et al(6) were used in the calculation of the collector efficiency function. Additional measurements at several wavelengths on chromium plates similar to the ones used in the collector confirmed the applicability of the theoretical reflectivity to our chromium surfaces. To simulate the effect of a line the value we used for the collector efficiency would have to be low by about a factor of two at .65keV. We feel that this large an error is unlikely. The other possible systematic error is an incorrect energy calibration of the proportional counter pulse amplitude response. The calibration is based on an irradiation of the counters with characteristic x-rays of .185, .282, .68 and 1.25keV several days before flight. One of the calibration points is very close in energy to the oxygen line. There are several indications from the flight data that the energy calibration is correct. A large increase in counting efficiency occurs below 0.28keV due to the K-edge of carbon in the detector window. In general the pulse height distribution reflects this feature. Errors in energy calibration would also distort other data as well as the Cygnus Loop. In the case of other events seen in this experiment both background data and another source, Cyg X-1, there are not indications of anomalies at 0.65keV, the energy of the line.

If we exclude the possibility that the spectral function is undergoing rapid changes in the wavelength interval of the observation, then the most likely form of the x-ray emission is radiation from a high temperature plasma. Hence the process responsible for the x-rays from the Cygnus Loop appears to be quite distinct from that of the Crab Nebula. This is not surprising in view of the large difference in age and volume between the objects. One now might consider the possibility that the large x-ray flux is responsible for the excitation of the optical line emission observed from the filaments of the Cygnus Loop. However, in the hot plasma hypothesis one encounters the difficulty of explaining the lack of consistency

between the high temperature observed in the x-ray region and the apparent low expansion velocity of the filaments.

We now know of two classes of x-ray sources among the supernova remnants -- the remnants of events that took place less than 10^3 years ago, and those more than 10^4 years old. Members of the first class, e.g., Crab Nebula, Tycho's Supernova, and Cas A are visible at energies above 2keV while members of the second class have been seen only below 1keV. The Cygnus Loop belongs to the second class and a recent report by Palmieri et al(10) adds Vela X and Puppis A to this class. The x-ray emission mechanism is known for only one member of the first class, the Crab Nebula and it is synchrotron radiation. Our results suggest that another mechanism, thermal radiation from a hot plasma, is responsible for the emission from the second class.

We acknowledge several informative discussions with Dr. W. Tucker of AS&E, and Dr. R. Angel of Columbia University. This work was supported by the National Aeronautics and Space Administration under Contracts NASW-1889 and NGR 33-008-102.

REFERENCES

1. R.J. Grader, R.W. Hill, J.P. Stoering, Ap. J. L45 (1970).

2. R.C. Henry, G. Fritz, J.F. Meekins, H. Friedman, E.T. Byram, Ap. J. 153, L11 (1968).

3. P. Gorenstein, B. Harris, H. Gursky, R. Giacconi, Nuc. Inst. and Meth. (In Press).

4. D.E. Hogg, Nebulae and Interstellar Matter, B.M. Middlehurst and L.H. Aller, Eds., The University of Chicago Press, Chicago (1968), Chap. II, Plate 4, 5.

5. P. Gorenstein, H. Gursky, G. Garmire, Ap. J. 153, 885 (1968).

6. O.A. Ershov, I.A. Brytov, A.P. Lukirskii, Opt. and Spect. 22, 66 (1967) (translated from Russian).

7. R. Minkowski, Rev. Mod. Phys. 30, 1048 (1958).

8. R.L. Brown and R.J. Gould, Phys. Rev. D 2252 (1970).

9. C.A. Heiles, Ap. J. 140, 470 (1964) and I.S. Shklovsky Supernovae John Wiley, New York (1968).

10. T.M. Palmieri, G. Burginyon, R.J. Grader, R.W. Hill, F.D. Seward, J.P. Stoering UCRL-72614 (1970).

Figure 1. Solid lines are the response of four independent proportional counter elements in focal plane during $1/4^{\circ}$/second scan across Cygnus Loop. Dotted lines represent response of instrument to point source at distance of 80 meters.

Figure 2. Total x-ray data from Cygnus Loop superimposed upon photograph of filaments taken in red light with 48-inch schmidt telescope (Mt. Wilson and Palomar Observatories). Field of view of the instrument is broad along direction of dashed lines.

Figure 3. The points are the pulse height distribution of counts from the Cygnus Loop as observed with this instrument. Smooth curves are the computed response of the instrument to expressions (a) and two cases of expression (b), B = O, and B finite. The line of sight density of interstellar hydrogen is included in the trial functions as a free parameter. Interstellar attenuation accounts for part of the turnover at low energies; the rest is instrumental.

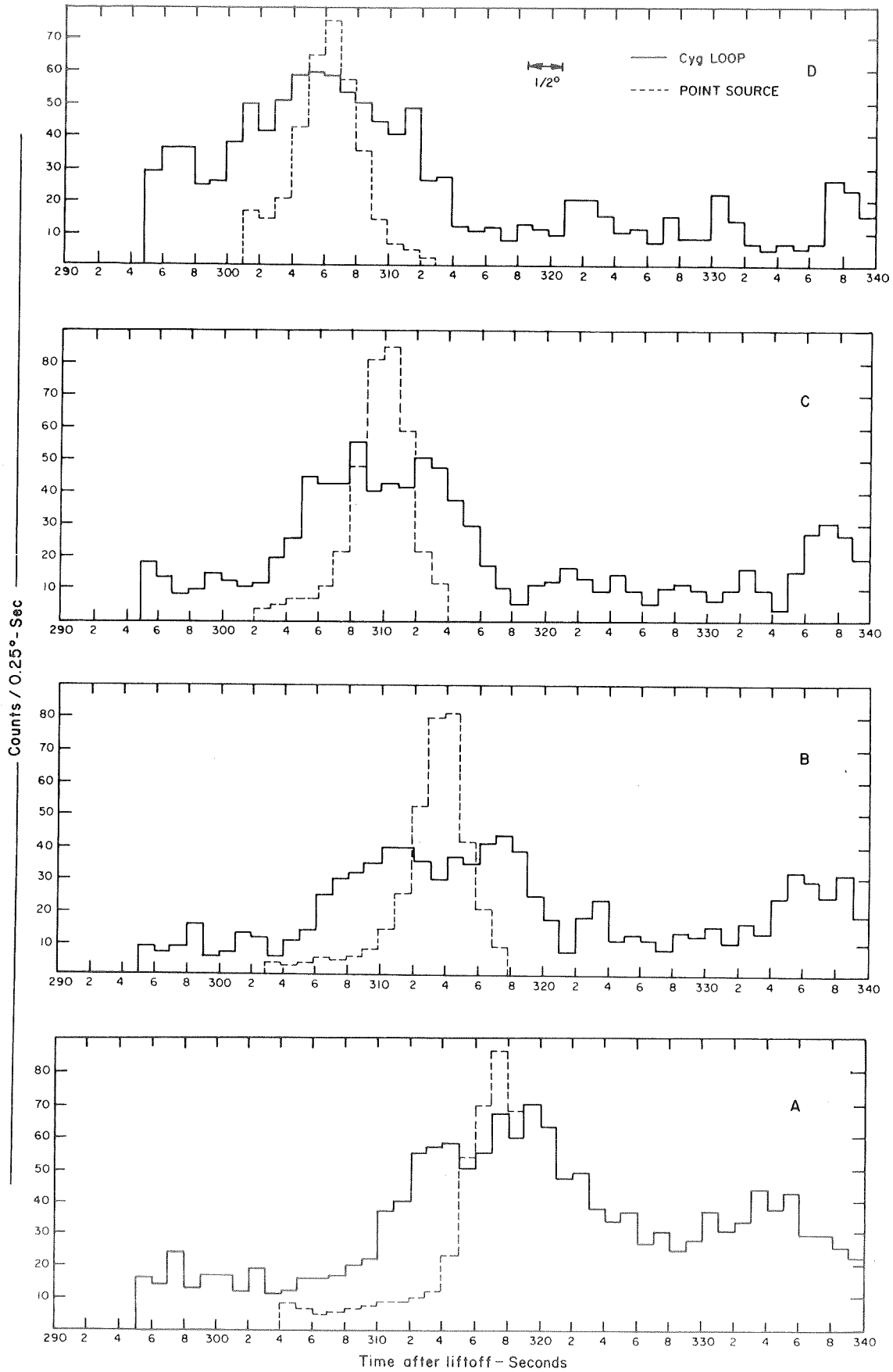
Cyg LOOP
POINT SOURCE
1/2°
D
C
B
A
Counts / 0.25°-Sec
Time after liftoff – Seconds

FIG. 1

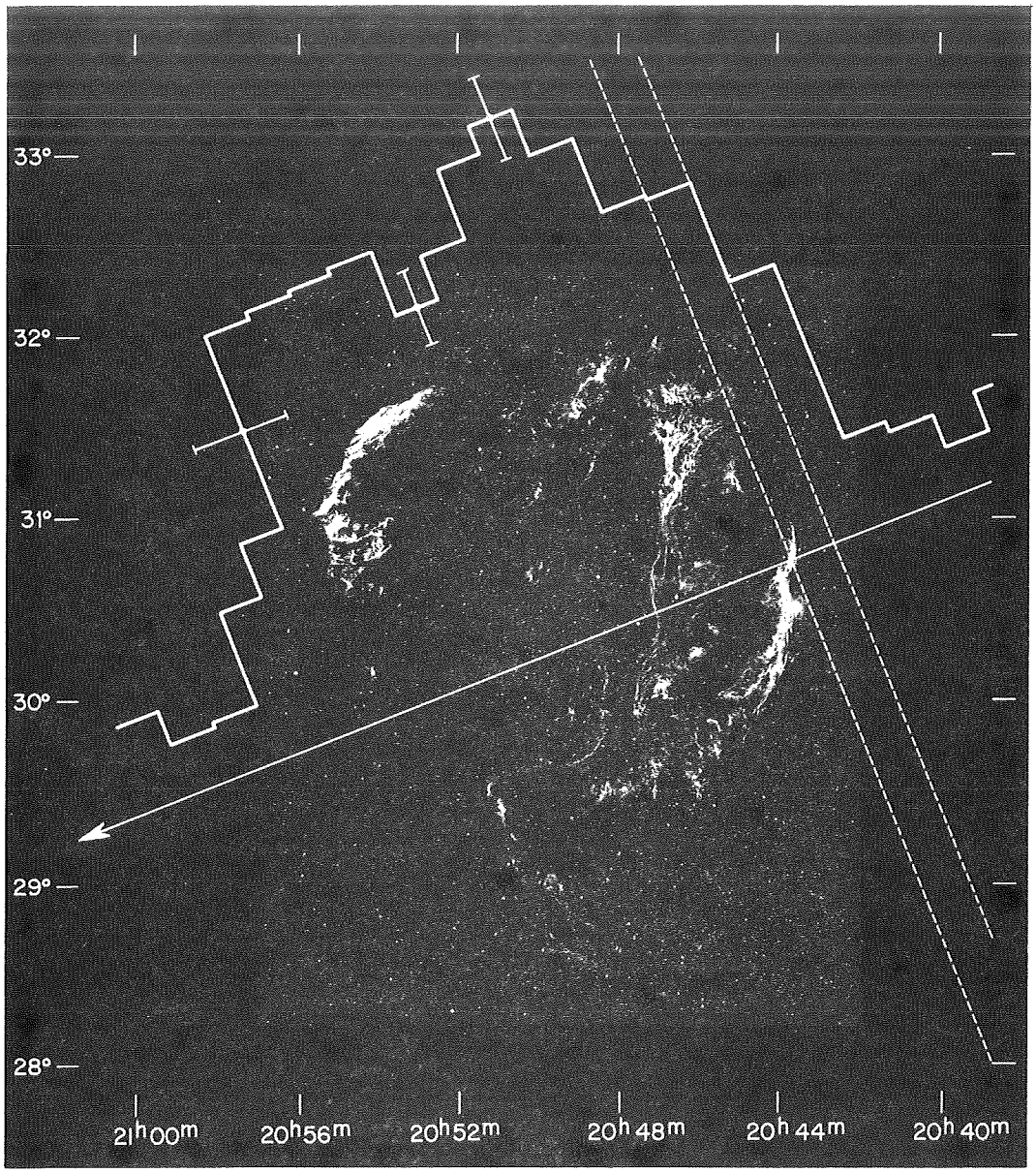

FIG. 2

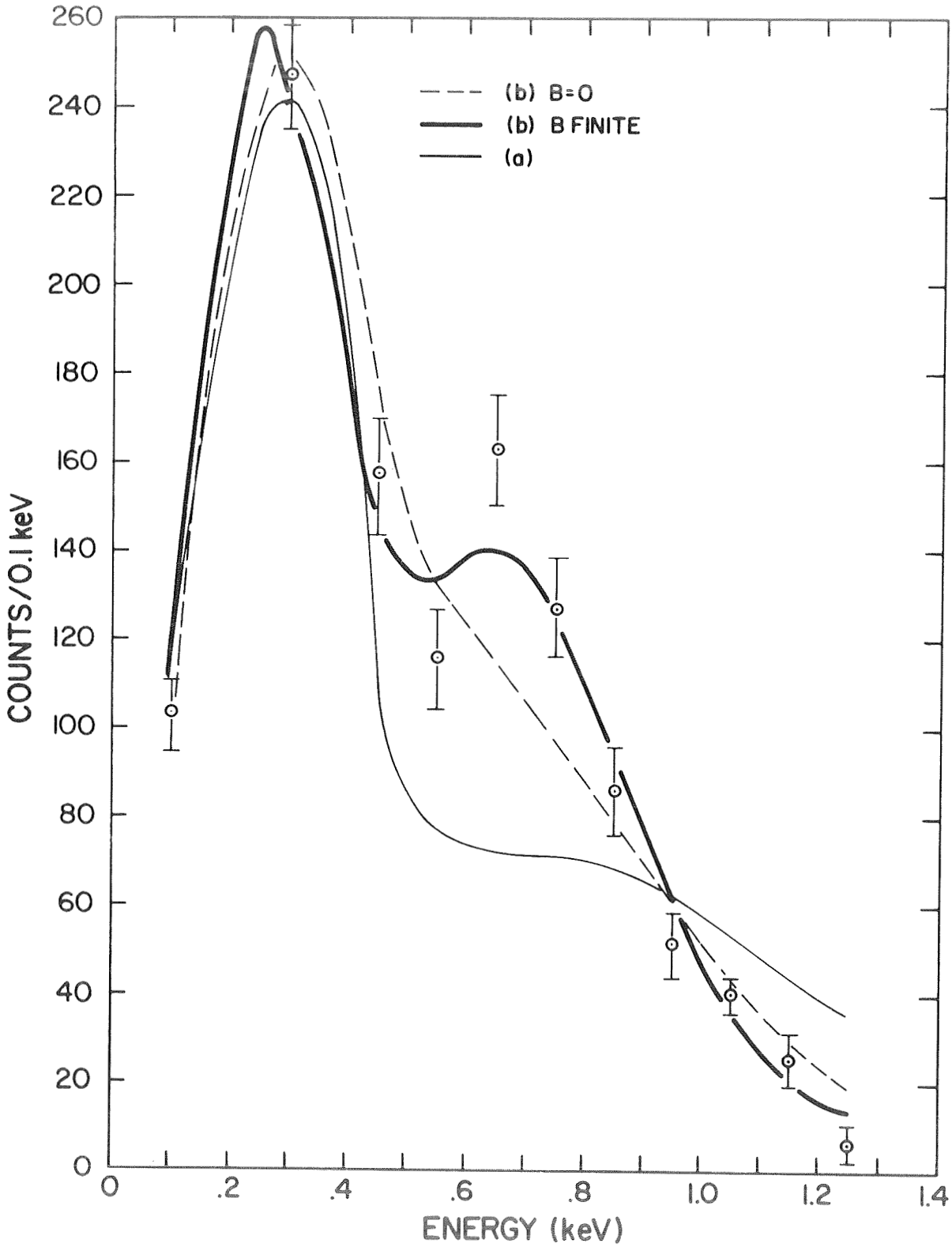
(b) B=0
(b) B FINITE
(a)
COUNTS/0.1 keV
ENERGY (keV)
0
20
40
60
80
100
120
140
160
180
200
220
240
260
0
.2
.4
.6
.8
1.0
1.2
1.4

FIG. 3

SECTION IV

PRELIMINARY COPY (still in preparation, figures not included)

ASE-2546

THE ESTIMATED DISTANCE TO CYG X-1 BASED ON ITS LOW ENERGY X-RAY SPECTRUM

H. Gursky and P. Gorenstein
American Science and Engineering
Cambridge, Massachusetts

F.J. Kerr and E.J. Grayzeck
Astronomy Program
University of Maryland
College Park, Maryland

ABSTRACT

Cyg X-1 was observed in the x-ray energy interval 0.2 - 1.2 keV with a focusing collector payload flown aboard a sounding rocket. The flux between 0.5 and 1.2 keV is consistent with the extrapolation of the power law spectrum observed at higher energies. Virtually no flux is seen below 0.5 keV, which is consistent with absorbing matter equivalent to 1.6×10^{21} H atoms/cm^2 along the line of sight. The 21 cm radiation profiles in the Cygnus region indicate that this amount of hydrogen represents a distance of about 1 kpc to the source. At this distance, the intrinsic luminosity of Cyg X-1 is about 10^{36} erg/sec between 0.5 to 100 keV.

I. INTRODUCTION

At the present time the only reliable distances that exist for cosmic x-ray sources are for well-known objects such as the supernova remnants. These distances are based on observations in the optical and radio wavelength regions. It has been known for some time that if an x-ray source is transparent to its own radiation, it is possible to determine the distance to an object by measuring the turnover in the low energy portion of its x-ray spectrum; this turnover presumably being caused by photoelectric absorption along the line-of-sight in the interstellar medium. The magnitude of the absorption is then relatable to N_H, the column density of hydrogen to the object. If N_H can be determined independently, and in the present case we do this by examining the 21 cm radiation profiles in the vicinity of the source, then the distance to the object is determined, or at least an upper limit to the distance, if some of the absorption is intrinsic.

As with most determinations in astronomy, this one is subject to great uncertainties. For example, the x-ray absorption takes place not in the hydrogen itself, but rather in the heavier elements - helium, oxygen, neon, etc. The value of N_H is obtained from the cosmic abundances, themselves only poorly known. This column density is then compared to a distance scale established from 21 cm emission which assumes the gas to be uniformly distributed and of uniform temperature.

It is also important to study the low energy spectrum of the cosmic x-rays for the information it gives regarding the object itself. Spectral lines, originating in the thermal bremmstrahlung process, may be more pronounced at the lower energies, or one may find changes in spectral shape indicating a fundamental feature of the process or possibly the onset of a new physical process.

II. X-RAY OBSERVATIONS

The x-ray observations were made with a "focusing collector" payload flown aboard an attitude controlled Aerobee 170 rocket on 26 June 1970. The instrumentation consisted of an assembly of chromium coated reflecting plates that focused a line image of a source upon a multiwire proportional counter having a 1.3 micron polypropylene entrance window. The sensitivity of the payload extended from 0.2 to 1.2 keV. The field of view of the collector was 2° in the direction of scan and 9° in the perpendicular direction. Its angular resolution in the scan direction was $1/2^{\circ}$. The instrumentation is described in detail in another publication (Gorenstein, Harris, Gursky, and Giacconi, 1970).

Cyg X-1 was observed for about a second as the rocket was performing a fast maneuver prior to scanning the Cygnus Loop. Although the aspect camera failed to record any stars during the fast maneuver an extrapolation of the rocket motion backward from the Cygnus Loop plus subsidiary data from the attitude control system restricts the position of the source to within 2° of Cyg X-1. The other known sources in Cygnus were outside of the field of view of the instrument at the time of the observation. These considerations plus the general consistency of the spectrum with measurements at higher energies leads us to conclude that the source is indeed Cyg X-1. The counting rates vs time are shown in Figure 1 for two intervals of proportional counter pulse height corresponding to approximately 0 - 0.5 keV and 0.5 - 1.2 keV in photon energy. The Cygnus Loop is seen in both energy intervals and these data are reported separately (Gorenstein et al, 1970). Cyg X-1 is seen only in the higher energy band.

A pulse height distribution totaling about one hundred net counts were obtained from Cyg X-1. It is possible to check the agreement of this distribution with a postulated spectral function. The source function based on a 2 - 10 keV observation of Cyg X-1 on 11 October 1966 (Gorenstein, Giacconi, and Gursky, 1967), is taken as,

$$dN/dE = 1.5\ (\pm .2)\ E^{-1.7 \pm .1}\ \text{photons/cm}^2\text{-sec-keV} \quad 2 - 10\ \text{keV} \qquad (1)$$

The error in the constant represents only that portion of the total error which is correlated with the 0.1 uncertainty in the spectral index. In addition there is an error in the constant of $\pm$ 8% representing uncertainties in statistics, live time, effective area, etc. The observations reviewed by Dolan (1970) plus a subsequent observation on Cyg X-1 (Grader, Hill, and Stoering, 1970) do not indicate any variability below 10 keV during recent years. The usual method of analysis was followed; the assumed source function is multiplied by all known efficiencies, convolved with the appropriate resolution response function of the proportional counter, and a histogram representing a pulse height distribution is computed. In addition, Equation 1 is multiplied by an x-ray transmission function appropriate for absorption in the interstellar material; namely,

$$T(E) = \exp -\left(\sum_i \sigma_i(E) N_i \right)$$

where $\sigma_i(E)$ is the photoelectric absorption coefficient for the ith element and Ni_ι is the column atoms cm^2 of that element. Following customary procedure, the sum is replaced by $\sigma_e(E)N_H$ where σ_e is the effective cross section assuming a particular mix of elements and N_H is the column density of hydrogen appropriate to that mix. N_H is left as a free parameter in the fitting. We have used the values of σ_e derived by Brown and Gould (1970). Helium, oxygen and neon are the principal absorbing elements for which Brown and Gould used log. abundances of 10.92, 8.95 and 8.00 respectively, relative to hydrogen (log abundance 12.00).* In the past, we have characterized interstellar attenuation by the energy, Ea, at which the optical depth is unity, which was then converted to N_H (Gorenstein, Giacconi, and Gursky, 1967). This is possible only when the absorption coefficient can be represented by the smooth function

$$\sigma = \sigma_o \, (E/Ea)^{-8/3}$$

*We have previously used σ_e calculated by Bell and Kingston (1967) which are based on neon abundances a factor of 2 higher; correspondingly, values of σ_e above the neon edge at 0.86 keV are about 30% higher than those of Brown and Gould.

as is the case at energies in excess of about 1 keV. At lower energies, oxygen produces a significant discontinuity in the absorption curve at an energy of 0.5 keV, which dominates the absorption in this region and makes it impossible to define Ea unambiguously.

The value of N_H that best fits the present data was $(1.6 \pm 0.4) \times 10^{21}$ H atoms/cm^2. The result is shown in Figure 2. The value of the chi-square indicates an acceptable fit; the error in N_H is taken as that amount which increases the minimum chi-square by one. The error does not include of course the systematic uncertainty resulting from possible errors in the interstellar absorption cross section. With this amount of absorbing matter the absolute intensity of Cyg X-1 is consistent within counting statistics with an extrapolation of Equation 1.

III. ESTIMATE OF DISTANCE

To convert the x-ray estimate of N_H to a distance, we can try to determine the column density of the interstellar hydrogen in the direction of Cyg X-1 by use of 21 cm observations. A distance scale, based on these observations, can be established, provided we assume that the gas is uniformly distributed in a spiral feature and of uniform temperature.

The only 21 cm profiles readily available to us in the approximate direction of the x-ray source are those published by Muller and Westerhout (1957). Figure 3 provides the positions of their profiles (numbers 3, 6, 7, and 10) and the positions of other interesting objects near Cyg X-1 such as the dark nebula L847, the bright nebula S101, and the bright star Cygni. We adopt the position of Cyg X-1 found by Giacconi et al (1967a), although the conclusions derived here are sensibly independent of the precise location of the source and we could have equally used the position found by Matsuoka et al (1970). We used the four available profiles to construct an interpolated profile at the x-ray source position, as shown in Figure 4. To interpret this brightness temperature-velocity profile, we adopted a model of the Cygnus feature (Figure 5) based on the distribution

of HI given by Kerr and Westerhout (1965), and used the rotation curve of Schmidt (1965) to deduce the velocity of the gas in the direction of Cyg X-1. This model indicates that hydrogen in the velocity range +20 to -10 km/sec can be detected to distances ~ 7 kpc within this spiral feature. The radiation from this gas is recognizable as the major peak at ~ +5 km/sec in the interpolated profile; radiation detected at large negative velocities appears to be due to more distant features. Thus we can construct a profile (the dotted line in Figure 4) for the hydrogen attributed to the Cygnus spiral arm within ~ 7 kpc and then calculate N_H from the equation

$$N_H = 1.8 \times 10^{18} B_{int}$$

where B_{int} is the area under the brightness temperature-velocity profile (^{o}K - Km/sec), and it is assumed that the gas is optically thin. Therefore, the calculated value for N_H, along the line of sight to Cyg X-1 within the Cygnus feature, is

$$N_H = 5.0 \times 10^{21} \text{ atoms/cm}^2.$$

If one assumes the hydrogen density to be uniform along the line of sight, a distance scale using the calculated 21 cm value for N_H can be established, but for calibration of the scale a further assumption about the gas distribution in the z direction is needed. Observational evidence actually indicates that the gas distribution is probably patchy across major spiral arms, within a spiral feature, and in the z direction. Nevertheless, if a uniform distribution is assumed and if the hydrogen layer follows a roughly gaussian shape in the z direction, as shown in Figure 6, then an average N_H for a particular line of sight can be calculated to the half-density points of the layer, which are typically at z distances of $\pm$ 100 pc from the galactic plane. With this z value and the latitude of the observed profile we can determine a linear distance, r, to the half density points,

which for Cyg X-1 is ~ 1.8 kpc. Since it is assumed that the gas layer in the z direction is in the form of a gaussian distribution, approximately 80% of the atoms are contained within the half density points along a specific direction. Consequently, for this x-ray source, only 4.0×10^{21} atoms/cm^2 ($0.8 \times 5.0 \times 10^{21}$ atoms/cm^2) lie within this distance, r. We conclude that a reasonable approximation to the N_H per kpc in the Cyg X-1 direction is 2.0×10^{21} atoms/cm^2-kpc. Combining this with the x-ray estimate of N_H along the line of sight (1.6×10^{21} atoms/cm^2) yields a distance to the object of ~ 0.8 kpc. A further check on this estimate is provided by the latitude variations of the 21 cm profiles at the longitude of the x-ray source. The Muller and Westerhout data indicate that N_H in the plane at this longitude within the Cygnus feature (a distance of ~ 7 kpc) is approximately twice the N_H found at the latitude of Cyg X-1. The N_H value calculated in front of the x-ray source (1.6×10^{21} atoms/cm^2) is approximately one sixth of that for the whole feature, implying a distance to the source ~ 1.0 kpc. Thus, the x-ray absorption data, combined with the 21 cm distance scale, formally yields a distance estimate to Cyg X-1 of 0.8 - 1.0 kpc.

As a test of this method of distance determination, we have repeated this procedure for three objects whose distances are known, the supernova remnants Cas A, SN1572 (Tycho), and the Crab Nebula. For these sources, which are both strong radio and x-ray emitters, preliminary x-ray absorption data and 21 cm studies allow a direct comparison of the derived N_H as shown in Table 1. N_H determined from x-ray information is taken from published data as noted and all numbers are based on the absorption coefficients of Brown and Gould. The N_H results from 21 cm emission were derived by us after integrating under the brightness temperature-velocity "expected" profiles constructed for the positions of the sources. The results are based on emission profiles obtained by Muller (1957), Shuter and Verschuur (1964), and Clark (1965), in the case of Cas A and Crab, and by Westerhour (1970) in the case of Tycho. The N_H values from 21 cm absorption in the

continuum emission are from published data with the exception that the value for Tycho is assumed to be the same as that for Cas A.

TABLE I

Source	N_H (atoms/cm^2)		
	X-ray Absorption	21 cm Emission	21 cm Absorption
Cas A	1.1×10^{22} (1)	0.45×10^{22}	1.0×10^{22} (4)
Tycho	$< 1.5 \times 10^{22}$ (1)	0.65×10^{22}	(1.0×10^{22})
Crab Nebula	$< 0.39 \times 10^{22}$ (1)	$< 0.35 \times 10^{22}$	0.16×10^{22} (4)
	0.25×10^{22} (2)		
	0.33×10^{22} (3)		

References for Table I

(1) Gorenstein, Kellogg and Gursky (1970)
(2) Grader, Hill, Seward and Hiltner (1970)
(3) Fritz, Meekins, Chubb, Friedman and Henry (1970)
(4) Muller (1957), and Clark (1965)

The agreement among the various N_H values for Cas A and Tycho is reasonable. From 21 cm absorption data, the derived parameter is the ratio N_H/T_s, where T_s is the gas spin temperature. A constant value of T_s, 100 or 125 K, has been used here to solve for the column density of hydrogen; however, present evidence indicates that some gas concentrations have T_s closer to 50 K. Consequently, N_H from these measurements can be considered an upper limit to the actual hydrogen column density. Conversely, the "expected" emission profile in the direction of a source yields a lower limit to N_H; if cold ($T_s \sim 50$ K) concentrations of gas where the optical depth exceeds unity occur along the line of sight, the radiation from atoms behind such clouds is not detected. The preliminary x-ray information for these two sources yields a value of N_H approximately within these limits.

A possible discrepancy of the N_H emission value for the Crab Nebula, which is 2.0 kpc away, may result from counting atoms not only in the Orion arm, but also in the more distant spiral features. From the profiles in this direction ($\ell = 184^{\circ}$), one cannot separate the gas in different spiral features and only an upper limit for N_H can be set, which could easily be high by a factor of two.

The reasonable agreement of the N_H values of Table 1 lend greater weight to the distance estimate for Cyg X-1. There are still large uncertainties in these calculations of distance. The need to interpolate a profile in the direction of Cyg X-1 introduces considerable error into the derived distance scale; consequently, we plan to observe the positions of this and other x-ray sources at 21 cm in the near future. The assumption that the hydrogen layer is uniformly distributed throughout the Cygnus feature is also questionable. Finally, the accuracy is limited by the existence of both hot (~ 1000 K) and cold (~ 50 K) gas components in a spiral arm, with differing optical depths, although we did find that the absorption and emission N_H values roughly bracketed the x-ray value.

IV. CONCLUSIONS

Using a distance to Cyg X-1 of 1.0 kpc, its luminosity in x-rays (0.5 - 100 keV) is about 10^{36} erg/sec, about a factor of ten below that of the Crab Nebula, but approximately the same as Cas A and the Tycho SN.

Because of the similarity of its spectrum to that of the Crab Nebula, it can be speculated that Cyg X-1 is a Crab-like object. However, we now find its intrinsic luminosity in x-rays to be substantially below that of the Crab. Also in radio, Andrew and Purton have placed an upper limit of 0.4 flux units at 4.6 cm on any emission from the region containing the source which is more than three orders of magnitude below the emission from the Crab. Furthermore, Floyd (1969) has placed an upper limit of 1.4' on the angular diameter for x-rays above 20 keV, which translates to a

linear diameter < 0.5 pc. This is substantially smaller than the known supernova remnants. Matsuoka et al (1970) have placed a less stringent limit on 3' on the source. Thus, if Cyg X-1 is to be considered a supernova remnant it must be very young to account for the small size.

Giacconi et al (1967a) failed to find an optical candidate for Cyg X-1. Specifically, there was no excessively blue object down to limiting magnitude of + 18 m within a 1° square field containing the source. Ignoring obscuration, an optical counterpart might be about + 16 m, if like Sco X-1, its optical continuum flux density equaled that observed at 0.5 keV. On the other hand, if the power law observed in x-rays extends into the optical range, the object would be of + 10 m. The heavy obscuration clearly present in the region could greatly modify the appearance of the object, either reddening it to the extent that it would not show a blue excess, or rendering it virtually invisible. However, our distance estimate does not exclude the possibility that Cyg X-1 is in front of much of this obscuration, which may be largely the result of the dark nebula Lynds 847 thought to lie between 0.5 - 1.0 kpc from us. If this is the case, the failure to find an optical counterpart implies that a great amount of self-absorption exists as has been observed in the infrared spectrum of Sco X-1 (Neugebauer, Oke, Becklin, and Garmire, 1969). This in turn implies that the x-ray absorption could be accounted for by material intimate to the source and the distance estimate derived here would only be an upper limit.

We would like to thank Dr. Andrew and Dr. Purton of the Radio and Electrical Division, National Research Council, Ottawa for allowing us to use unpublished radio continuum observations on Cyg X-1. Several discussions with R. Giacconi and W. Tucker of ASE are gratefully acknowledged. This work was supported by the National Aeronautics and Space Administration under contract NASW-1889 and the NSF under grant GP-18626.

REFERENCES

Andrew, B., and Purton, C. 1970 (Private Communication).

Bell, K.L., and Kingston, A.E. 1967, Mon. Not. R. Ast. Soc. 136.

Brown, R., and Gould, R. 1970, Phys. Rev. D. 1, 2252.

Clark, B.G. 1965, Ap. J. 142, 1398.

Dolan, J.F. 1970, Space Science Reviews 10, 830.

Floyd, F. 1969, Nature 222, 967.

Fritz, G., Meekins, J.F., Chubb, T.A., Friedman, H., and Henry, R.C., "The X-ray Spectra of the Crab Nebula and NP0532", Preprint, January 1971.

Giacconi, R., Gorenstein, P., Gursky, H., and Waters, J.R. 1967a, Ap. J. 148, L119.

Giacconi, R., Gorenstein, P., Gursky, H., Usher, P., Waters, J.R., Sandage, A., Osmer, P., and Peach, J. 1967b, Ap. J. 148, L129.

Gorenstein, P., Giacconi, R., and Gursky, H. 1967, Ap. J. 150, L85.

Gorenstein, P., Harris, B., and Gursky, H. 1970, Nuc. Inst. and Mech. (In Press).

Gorenstein, P., Kellogg, E.M., and Gursky, H. 1970, Ap. J. 160, 199.

Gorenstein, P., Gursky, H., Giacconi, R., Novick, R., and Vanden Bout, P. 1970, Presented at Brighton I. A. U. Assembly, August (to be published).

Grader, R.J., Hill, R.W., Seward, F.D., and Hiltner, W.A. 1970, Ap. J. 159, 201.

Grader, R., Hill, R., and Stoering, J. 1970, Ap. J. 161, L45.

Kerr, F.J., and Westerhout, G. 1965, Stars and Stellar Systems, Vol. V, Ed., Blaauw and Schmidt, Ch. 9.

Matsuoka, M., Miyamoto, S., Nishimura, J., Oda, M., Ogawara, Y., and Wada, M. 1970, Non Solar X- and Gamma-Ray Astronomy (L. Gratton, Ed.) 130-133, I. A. U. Assembly.

Muller, C.A. 1957, Ap. J. 125, 830.

Muller, C.A., and Westerhout, G. 1958, B. A. N. 13, 151.

Neugebauer, G., Oke, J.B., Becklin, E., and Garmire, G. 1969, Ap. J. 155, 1.

Schmidt, M. 1965, Stars and Stellar Systems, Vol. V, Ed., Blaauw and Schmidt, Ch. 22.

Shuter, W.L.H., and Verschuur, G.L. 1964, M. N. 127, 387.

Westerhout, G. 1970 (Private Communication).